Document downloaded from:

http://hdl.handle.net/10251/197955

This paper must be cited as:

Merelo Cremades, P.; González-Cuadra, I.; Ferrandiz Maestre, C. (2022). A cellular analysis of meristem activity at the end of flowering points to cytokinin as a major regulator of proliferative arrest in Arabidopsis. Current Biology. 32(4):749-762. https://doi.org/10.1016/j.cub.2021.11.069

The final publication is available at

https://doi.org/10.1016/j.cub.2021.11.069

Copyright Elsevier

Additional Information

A cellular analysis of *Arabidopsis* meristem activity at the end of flowering points to cytokinin as a major regulator of proliferative arrest

Paz Merelo[1, *], Irene González-Cuadra[1] and Cristina Ferrándiz[1, 2, *]

[1] Instituto de Biología Molecular y Celular de Plantas, CSIC-UPV, 46022 Valencia, Spain

[2] Lead Contact

* Correspondence: pmerelo@ibmcp.upv.es, cferrandiz@ibmcp.upv.es

Summary

In monocarpic plants, all reproductive meristem activity arrests and flower production ceases after the production of a certain number of fruits. This proliferative arrest (PA) is an evolutionary adaptation that ensures nutrient availability for seed production. Moreover, PA is a process of agronomic interest because it affects the duration of the flowering period and therefore fruit production. While our knowledge of the inputs and genetic factors controlling the initiation of the flowering period is extensive, little is known about the regulatory pathways and cellular events that participate in the end of flowering and trigger PA. Here, we characterize with high spatiotemporal resolution the cellular and molecular changes related to cell proliferation and meristem activity in the shoot apical meristem throughout the flowering period and PA. Our results suggest that cytokinin (CK) signaling repression precedes PA, and that this hormone is sufficient to prevent and revert the process. We have also observed that repression of known CK downstream factors such as type B cyclins and WUSCHEL (WUS) correlates with PA. These molecular changes are accompanied by changes in cell size and number likely caused by the cessation of cell division and WUS activity during PA. Parallel assays in *fruitfull* (*ful*) mutants, which do not undergo PA, have revealed that FUL may promote PA via repression of these CK-dependent pathways. Moreover, our data allow to define two phases, based on the relative contribution of FUL, that lead to PA: an early reduction of CK-related events and a late blocking of these events.

Introduction

Monocarpic plants need to tightly regulate the timing and duration of the flowering period to ensure reproductive success, and this involves not only to flower at most advantageous conditions, but also regulating the end of the flowering phase to complete fruit filling and redirect nutrients for optimal seed production before plant death. The end of flowering is characterized by a sharp cessation of meristem activity, a proliferative arrest that has been described in several distant species[1–3]. In *Arabidopsis thaliana*, proliferative arrest is visible as an apical cluster of arrested floral buds, below which fertilized fruits complete their development (Figure 1).

Decades of genetic and molecular work have generated a vast knowledge of the endogenous and exogenous cues that control flowering time in *Arabidopsis* and many other species[4,5–8]. In marked contrast, and despite its ecological and economical importance, the controlled termination of the flowering phase has been a neglected topic for years. Several physiological studies in the last century described the phenomenon of proliferative arrest at the end of the flowering phase. These studies showed a major role of seed production in proliferative arrest timing[1–3]. In sterile plants, proliferative arrest is delayed or even prevented, as it occurs in *Arabidopsis*, where the inflorescence meristem produces a large number of flowers before differentiating into a terminal flower in the absence of seeds[1]. These early works also suggested the existence of a graft-transmissible signal coming from fruits and of genetic factors that control proliferative arrest timing, but failed to identify such factors. Only recently, the interest in this process has been rekindled with new studies in *Arabidopsis* that have uncovered some components of the mechanisms involved in triggering proliferative arrest. Thus, an age-dependent genetic pathway controlling proliferative arrest has been identified that involves the transcription factors FRUITFULL (FUL) and APETALA2 (AP2)[9,10], which regulate the expression of *WUSCHEL* (*WUS*), a major meristem function regulator[11–13]. Moreover, detailed transcriptomic analyses of this developmental process have revealed that the arrested meristem behaves as a dormant meristem[14] and that AP2 is involved in the induction of this dormant state by regulating genes related to hormonal and environmental responses[15]. These works also indicate that proliferative arrest is a reversible process and that meristem activity can be restored either by fruit removal, as previously shown[1], or by inducing AP2 expression in the meristem. Finally, it has been shown that this process is locally regulated within individual inflorescences, which are arrest-competent only after reaching a certain developmental age, and that auxin exported from the last developing fruits could trigger meristem arrest by altering auxin canalization in the stem[16]. A recent work[17] proposes that the effect of fruits on proliferative arrest is mediated by changes in auxin transport and signaling in the apical region of the stem as well as by changes in sugar signaling and metabolism in the shoot apex. However, this new information is still scattered and difficult to integrate into a coordinated temporal and spatial framework with an accurate description of the meristem dynamics at or around proliferative arrest. In this work, we aim to fill this crucial gap by characterizing histological changes, cell division patterns and meristem activity markers in the shoot apical meristem (SAM) during advanced flowering stages and proliferative arrest. We also make use of *ful* mutants, which do not undergo proliferative arrest, but display a gradual decrease of floral production until the death of the plant, to better understand the specific cell signatures associated with the abrupt arrest of meristem activity and to get further insights on the role of FUL in the process. Our results have allowed to differentiate two phases at the end of the flowering period leading to proliferative arrest. Initially, a reduction of CK signaling and CK-downstream factors such as cell division regulators or WUS occurs, where FUL would play a role together with additional elements. Secondly, a complete repression of these CK-related factors strongly dependent on FUL would block meristem activity and ultimately results in proliferative arrest.

Results

Proliferative arrest correlates with a decrease of cell size and cell number within the shoot apical meristem

Quantification of flower and fruit production during advanced flowering stages until the onset of proliferative arrest allowed to distinguish two different phases preceding proliferative arrest. First, a high proliferation phase where the shoot apex at a defined time point showed an elevated number of open flowers (1-3 wab), and that correlated with a fast rise of the total number of mature fruits in the main stem up to 4 wab. Second, a transition phase (4-5 wab) where the rate of flower production rapidly decreased, and that translated into a slower rate of fruit accumulation (Figure 1A). Then, proliferative arrest occurs and normally is visible between 4-5 wab, when the characteristic terminal cluster of non-developing flower buds is formed[1] (Figure 1B). After proliferative arrest, no flowers are produced. These kinetics suggested that the meristem activity is already changing quite in advance of the observation of the arrested inflorescence. This prompted us to define in an accurate way the sequence of cellular and molecular events leading to proliferative arrest to better understand the role of different factors that have been previously related to meristem activity regulation.

Dynamic changes in the stem cell and SAM size have been studied mostly at specific developmental stages, such as floral transition and shortly after bolting, or during short time lapses[18–21]. Previous works have also shown that cell number and size and the total SAM size increase during floral transition[8,22–25]. However, it remains unknown whether changes in cell size and number within the SAM could be related to the onset of proliferative arrest. Therefore, we quantified these parameters and the SAM area in active and arrested SAMs using MorphoGraphX[26], which allowed to delimit the meristem region (Figure S1) and perform 2.5D segmentation of L1 cells.

Our analyses revealed a significant decrease in cell size, cell number and SAM size 3 wab, and these parameters continued decreasing at a lower rate until the meristem arrest (5 wab) (Figures 1C-1F). The decrease of these parameters correlated with the gradual decline of flower production and deceleration of fruit production (Figure 1A). As mentioned before, previous studies have shown that fruit pruning after the proliferative arrest onset reactivates arrested SAMs[1,14,16]. Based on this evidence, and to test whether the changes in SAM size correlated with the changes in its activity and, therefore, potentially with proliferative arrest, we segmented SAMs one and two weeks after reactivation by pruning (wap) (6 and 7 wab, respectively, since plants were pruned 5 wab, when the proliferative arrest was observed). Fruit removal caused a dramatic increase in the SAM area, mainly associated with the increase in cell area, specially 1 wap (Figures 1C, 1D and 1F), correlating with the reactivation of organ formation (Figure 1B), but decreased one week later. However, cell number increased to a lesser extent at 6 wab than cell area and meristem area (Figure 1E). Reactivated

apices showed a smaller SAM size and a lower cell number in comparison with highly active apices (2 wab), and produced a few flowers and fruits before arresting again. This suggested that the size acquired by the SAM at the meristem arrest moment, and particularly the number of cells within the SAM, conditions SAM activity. Altogether, these results suggest that SAM size reduction is a limiting factor of SAM activity along the progression of the flowering period and establishes it as determinant for proliferative arrest. Moreover, since such changes started considerably prior to proliferative arrest (3 wab), they point towards the existence of early and gradual programmed mechanisms controlling this process.

Proliferative arrest involves repression of cell division

Previous works have proposed that changes in cell size in the SAM are a consequence of altering cell growth and division rates[19,21]. Cell division implies a previous step of DNA replication, which results in cell growth. Then, after mitosis, daughter cells grow during the differentiation process[18–20,27]. To assess with detailed spatiotemporal resolution whether the decrease in cell size and number depends on the decline of cell divisions within the SAM and, in turn, whether proliferative arrest depends on changes in cell division patterns, we generated a fluorescent reporter for cell division and monitored its expression in the shoot apex along the reproductive phase up to proliferative arrest. This marker was based on the published cyclinB1;2-GUS reporter (CYCB1;2)[28]. Type B cyclins are expressed during the G2/M (post-synthesis gap 2/mitosis) transition and degraded at the end of anaphase via the ubiquitin-proteasome system[29]. In particular, to visualize cell divisions in the SAM, we used the *CYCB1;2* destruction box (Dbox; a N-terminal motif that acts as a target for degradation) fused to GFP and expressed under the *CYCB1;2* promoter (*CYCB1;2$_{pro}$:Dbox-GFP*, CYCB1;2-GFP).

Active SAMs 2 wab contained a high number of CYCB1;2-GFP expressing cells that were more densely located in the developing primordia (P1-P5; Figures 2A, 2F and 2K), but also in the central zone (CZ) and, particularly, in the incipient primordia (I1; Figures 2A and 2F). CYCB1;2-GFP expressing cells were also detected at the meristem-primordia boundaries of young primordia (around P1-P3) (red arrowheads; Figure 2F), indicating active primordia formation at this stage[30–32]. One week later (3 wab), CYCB1;2-GFP expression was mainly restricted to a few cells in some primordia, being undetectable in the CZ, incipient primordia or boundaries (Figures 2B, 2G and 2K). This observation correlated with the start of the flower production decline (Figure 1A), suggesting that probably around one week before the conspicuous meristem arrest no new primordia were initiated. Lastly, no CYCB1;2-GFP signal was observed in arrested apices (Figures 2C, 2H and 2K). In addition, CYCB1;2-GFP expression was rapidly restored one day after pruning (dap) and maintained longer (1 wap) (Figures 2D, 2E, 2I, 2J and 2K). The gradual changes in cell division frequency tightly matched with the changes in histological parameters along advanced flowering stages, proliferative arrest and meristem reactivation (Figures 2 and 1C-1F). Indeed, segmentation

of active and reactivated SAMs of CYCB1;2-GFP transgenic lines showed that a high proportion of bigger cells corresponded to cells in mitosis (Figure 2L), which were mainly observed at the young or incipient primordia and meristem-primordia boundaries (yellow, black and white asterisks; Figure S2). Therefore, these data confirmed our previous assumption: proliferative arrest entails repression of cell division and growth events and, thus, cell cycle progression.

These results are in agreement with previous transcriptomic studies that reported low expression levels of cell cycle-related genes in arrested meristems and high levels after fruit removal[14]. In line with this work, our results demonstrate that proliferative arrest represents a reversible mitotic dormancy stage, instead of being a mitotic senescence process[3,33,34]. Furthermore, our data indicate that repression of cell division constitutes an early and gradual cellular mechanism controlling proliferative arrest. Firstly, cell divisions are repressed in the CZ of the SAM, where normally meristematic cells divide slowly and part of the progeny is incorporated into the peripheral zone (PZ). Secondly, cell divisions are repressed in the PZ, where cells divide fast and differentiate to form new organs[35–37]. This leads to interesting questions to be addressed in the future about whether different factors may regulate meristem arrest in a spatial-dependent manner.

Cytokinin signaling repression precedes proliferative arrest

Cytokinins (CKs) stimulate the proliferative capacity of the SAM[38–40] and promote mitotic division through the regulation of G1/S and G2/M transitions and different cell cycle components, such as CYCB, CYCD, Cyclin-Dependent Kinases (CDK), or the recently reported MYB-DOMAIN PROTEIN 3R4 (MYB3R4)[38,41–43]. These studies together with the connection between repression of CYCB1;2 and proliferative arrest led us to investigate in detail how the CK dynamics correlates with SAM activity and the proliferative arrest, and try to identify a potential relationship between them. For this, we analyzed the CK fluorescent sensor *TCSn:GFP-ER* (Two Component signaling Sensor new)[44,45], which provides a readout of CK signaling and indirectly of CK levels, in active, arrested and pruning-reactivated shoot apices.

Visualization of active apices 2 wab revealed a high TCSn signal in the organizing center (OC) and in the center of developing flower primordia (Figures 2M and 2R). Also, detailed visualization of meristem-primordia boundaries at certain developmental stages (around P1-P3) revealed TCSn expression in boundary cells (Figure S3). In SAMs 3 wab, TCSn expression decreased to very low levels both in the OC and in the flower primordia (Figures 2N and 2S). The reduction of CK signaling correlated with the first signs of decline in flower and fruit production (Figure 1A). Finally, TCSn signal was almost undetectable in arrested SAMs and primordia 4 wab (Figures 2O and 2T) and was restored rapidly after pruning (1 dap) and maintained longer (1 wap) at levels similar to prearrested meristems (Figures 2P, 2Q, 2U and 2V). These results suggest that the repression of CK perception and signaling, and probably an extreme reduction in CK levels, trigger proliferative arrest. Moreover, the gradual repression of CK signaling and its recovery after pruning strongly correlated with the

changes in CYCB1;2-GFP expression in the shoot apex. In addition, early reactivated apices (1 dap) exhibited TCSn signal at the meristem-primordia boundaries, correlating with the recovery of cell divisions at this domain as well (white and red arrowheads; Figures 2I, 2P and 2U). Altogether, our data suggest that both CK signaling and CK-dependent cyclins are likely part of the same sequence of events involved in the early control of proliferative arrest. This correlation is also connected to parallel changes in cell size and number in the SAM (Figures 1C-1F), which is in agreement with previous studies showing that defective CK signaling or reduced CK levels lead to smaller meristems with fewer cells[46–48], while increased endogenous CK levels result in enlarged meristems with a higher number of cells[39,40]. Finally, rapid reactivation of CK signaling after fruit pruning (seed removal), together with the evidence that seed-derived signals control proliferative arrest[1,14,16], suggest that such signals may regulate the process through CK-related pathways.

Cytokinins prevent proliferative arrest and reactivate arrested meristems

To gauge the relative importance of CKs on the maintenance of SAM activity along the flowering period and, specially, on proliferative arrest, we treated active apices from 2 wab, and continuously (every 3 days), with CKs (100 μM N6-benzylaminopurine, BAP) and mock (control), as well as arrested apices (4 wab). Plants continuously treated with BAP were still active 5 weeks after the initial treatment (wat) (or 7 wab), while control plants stopped to produce flowers 2 wat (or 4 wab) (Figures 3A-3D). In fact, BAP-treated apices did not undergo proliferative arrest until the treatment was stopped. We also compared the expression pattern of TCSn in BAP-treated and control apices. TCSn expression was almost undetectable in arrested apices of control plants 2 wat (Figures 3E and 3H), while apices of BAP-treated plants showed high levels of TCSn signal and an expanded TCSn expression domain (Figures 3F and 3I). TCSn expression levels remained high until the end of BAP treatment (5 wat; Figures 3G and 3J). In addition, BAP-treated apices showed a bigger SAM with a higher number of cells and flower primordia in comparison with control plants (Figures 3E-3J). These observations correlate with previous works describing that exogenous application of CKs is sufficient to expand CK signaling to cells out of the OC in the SAM[49] and to increase meristem size due to CK-promoted cell division[43]. In addition, they support our previous hypothesis that the onset of proliferative arrest could be a consequence of SAM size reduction, which would be in turn a consequence of very low levels of CKs, a marked reduction in CK signaling and the subsequent cell division cessation in the SAM.

Notably, arrested apices treated with BAP (4 wab) were reactivated and produced new buds and flowers 1 wat, while mock-treated apices remained arrested (Figures 3O and 3T). In these plants, TCSn expression was restored in the OC, primordia and boundaries one day after treatment (dat) (Figures 3P and 3Q), indicating an early reactivation of CK signaling and SAM function that was maintained 1 wat (Figures 3R and 3S). As expected, in control SAMs TCSn signal was very low or undetectable 1 dat and 1 wat (Figures 3K-3N). Overall, these assays clearly indicate that CKs are

sufficient to maintain SAM activity indefinitely, preventing proliferative arrest, and to revert this process.

Our results are in line with a previous study[15] showing that AP2, a regulator of proliferative arrest[9], promotes SAM activity at least in part by negatively regulating the *KISS ME DEADLY1* (*KMD1*), *KMD2* and *KMD4* genes[50], which repress the Type-B ARR genes and therefore CK response[51–53]. Interestingly, our detailed live imaging assay showed that CK signaling repression constitutes an early molecular mechanism controlling this process. Furthermore, prevention and reversion of meristem arrest by CKs strongly link these hormones with the negative control of proliferative arrest.

WUSCHEL repression in the SAM correlates with the CK signaling temporal pattern during proliferative arrest

CKs are critical for the maintenance of SAM activity by regulating the expression of *WUS*[54]. In particular, Type-B ARRs induce *WUS* expression in the presence of CK. In turn, WUS directly represses *Type-A ARRs*, the repressors of the CK signaling pathway, leading to a positive CK-WUS feedback loop[49,55]. *WUS* transcription is not detected at proliferative arrest [9], indicating a strong correlation with this process, but the precise dynamics of WUS protein accumulation patterns around proliferative arrest are unknown, as well as how changes in CK signaling correlate with changes in WUS expression. For this purpose, we monitored with detailed spatiotemporal resolution the expression of the translational reporter WUS_{pro}*:eGFP-WUS* (GFP-WUS)[56]. GFP-WUS was highly expressed in the OC and in the center of developing primordia of active apices 2 and 3 wab (Figures 4A, 4B, 4F and 4G). Subsequently, GFP-WUS protein levels decreased rapidly from 3 wab (Figure S4), being restricted to a few cells within the OC, up to proliferative arrest (4 wab), when GFP-WUS expression was undetectable (Figures 4C and 4H). Therefore, WUS protein repression started shortly after the CK signaling decrease rather than a week later. On the other hand, after reactivation of arrested apices by pruning, GFP-WUS expression was restored in the OC and primordia 1 dap (Figures 4D and 4I) and was maintained 1 wap (Figures 4E and 4J), resembling TCSn intensity and temporal distribution (Figures 2M-2V).

WUS is required for maintaining the stem cell niche in the SAM. The SAMs of *wus* mutants terminate after producing a few organs due to stem cell exhaustion[12]. Moreover, WUS maintains stem cell homeostasis by controlling stem cell number and rates of cell division and differentiation in the SAM. Thus, elevated levels of WUS promote expansion of the CZ, and also lead to increased cell division rates in the PZ, whereas a reduction of WUS levels lead to a smaller CZ and a reduction in cell division rates[57]. Our data revealed a decrease in the number of cells in the L1 layer of the meristem region (Figures 1C and 1E). Therefore, the reduction in SAM size could be a consequence of repression of CK-dependent cell division and growth, as we previously described, but also of WUS activity repression. Proliferative arrest would then represent a process of stem cell exhaustion. Moreover, the correlation between WUS expression and temporal patterns of CK distribution

suggests that the CK-WUS pathway is affected during proliferative arrest and it constitutes an early molecular mechanism that regulates this process together with other CK-dependent pathways.

FRUITFULL is involved in the repression of CK-dependent processes

Besides defining the dynamic changes related to stem cell proliferation and meristem activity involved in proliferative arrest, we aimed to assess the relative importance of these factors on the regulation of the process itself. We made use of *ful* mutants, which do not undergo proliferative arrest (Figures 5A and 5B) and produce flowers and fruits indefinitely, even when most of the body plant is in an advanced senescent stage (Figure S5). Therefore, this genetic background may help to define required events leading to proliferative arrest and also to investigate further the mode of action of FUL, a key regulator of the process[9].

Quantification of flower and fruit production along the reproductive period (2-7 wab) showed that *ful* mutants behaved similarly to wild-type plants up to 5 wab (Figure 5A), which corresponds approximately to the onset of proliferative arrest in wild-type. However, *ful* mutants did not arrest but continued producing flowers 5 wab. Subsequently, these plants entered into a third phase, producing flowers beyond this time point, although at a much lower rate (low proliferative phase; 6-7 wab) (Figures 5A and 5B).

Segmentation of *ful* mutants throughout the reproductive period revealed similarities and differences with wild-type SAM behaviour (Figures 5C-5F). Cell area, cell number and SAM area decreased similarly to wild-type until 5 wab (proliferative arrest onset in wild-type). Strikingly, after this time point (5 wab), cell area in non-pruned fertile *ful* mutants increased at 6-7 wab mimicking the response of arrested wild-type meristems that were reactivated by fruit pruning (Figures 5C and 5D). In contrast, cell number and SAM size in *ful* mutants decreased more than in reactivated wild-type meristems at 6 wab. Later, all parameters were almost equal in both genetic backgrounds (non-pruned *ful* and reactivated-by-pruning wild-type) at 7 wab (Figures 5D-5F).

Monitorization of cell division with CYCB1;2-GFP in *ful* apices showed a decrease in the frequency of divisions 3 wab, as in wild-type apices, and specially between 4 and 5 wab, when CYCB1;2-GFP expression was restricted to some cells in the incipient or young primordia (Figures 6A-6F and 6I). However, cell divisions were not completely repressed in *ful* (Figures 6C-6F and 6I) as in arrested wild-type apices 5 wab (Figures 2C, 2H and 2K). The number of dividing cells augmented 6 wab in the SAM and also in the meristem-primordia boundaries of non-pruned *ful* plants (Figures 6G and 6I), as in reactivated wild-type apices (Figures 2D, 2E, 2I, 2J and 2K), and was maintained 7 wab (Figures 6H and 6I). TCSn pattern in *ful* SAMs also showed similarities and differences with that in wild-type apices. The signal of the TCSn sensor decreased in *ful* SAMs 3 wab in comparison with SAMs 2 wab as in wild-type SAMs (Figures 6J, 6K, 2M, 2N, 2R and 2S). However, it was still detectable 4 wab (Figure 6L), unlike in arrested wild-type SAMs (Figures 2O and 2T), and 5 wab

(Figure 6M). Interestingly, TCSn expression increased 6 wab in the CZ and the meristem-primordia boundaries (Figure 6N) as in reactivated wild-type SAMs (Figures 2P and 2U). TCSn expression was still maintained 7 wab (Figure 6O). Finally, *ful* meristems maintained GFP-WUS expression throughout the reproductive phase (2-7 wab) (Figures 6P-6U), correlating with the indeterminate SAM activity displayed by these mutant plants. GFP-WUS signal declined moderately in *ful* apices from 3 to 5 wab (Figures 6Q, 6R and 6S) but, again, increased 6 and 7 wab as in reactivated wild-type apices (Figures 6T, 6U, 4E and 4J).

The described reduction in the flower production rate in *ful* plants from 3 to 5 wab (Figure 5A) was in agreement with the observed decline in CK signaling, WUS expression and cell division, as well as the consequent reduction in cell size, cell number and SAM size. Also, and differently from arrested wild-type apices, the absence of a complete blocking in CK signaling, cell cycle progression and WUS activity explained that *ful* mutants did not experience proliferative arrest and continued producing flowers. However, *ful* plants continued producing flowers at a very low rate 6-7 wab, which did not correlate with the increase in CK signaling, WUS expression, cell divisions and cell area observed in *ful* SAMs 6-7 wab in comparison with previous time points (4-5 wab). A possible explanation for this apparent contradiction could be related to the relatively small size of the *ful* SAM at 6 wab, which despite displaying high indicators of cell division activity, could not support enough differentiation rates. This indicates again that below a certain threshold in cell number and SAM size the meristem proliferative capacity is affected and, probably, cell proliferation at the CZ cannot compensate organ differentiation and outgrowth at the PZ of the SAM. In addition, besides the proposed influence of SAM size as a limiting factor for proliferation, the presence of seed-derived signals[1–3] still active in non-pruned *ful* mutants or additional factors could also contribute to the observed SAM behavior.

A second conclusion can be also extracted from these results. The transient decrease of CK signaling, WUS protein levels and cell division and growth (3-5 wab) in *ful* apices is similar to wild-type apices from 3 wab to the proliferative arrest, but it never gets totally blocked. The slightly higher levels of CK signaling, WUS expression and cell divisions from 3 wab indicate that FUL participates, at least partially, in the negative regulation of these processes before the onset of proliferative arrest. However, the maintenance of these basal levels 4-5 wab, in contrast to their complete repression in wild-type plants at proliferative arrest, strongly suggest that FUL is required for providing a robust shutdown of the meristem activity. Moreover, the increase in CK signaling, WUS expression and cell divisions observed in *ful* SAMs at late stages (6 and 7 wab) may indicate the existence of a critical time point at which FUL may play a major role on the repression of these CK-related events, when the characteristic arrested inflorescence is visible. It remains to be understood the mechanism for this late repressive activity of FUL. Interestingly, previously published ChIP-seq data[58] demonstrated that FUL directly activates the expression of the *CYTOKININ OXIDASES CKX3* and *CKX5*, which encode enzymes involved in CK degradation[59,60]. These studies together with our data lead us to

hypothesize that repression of CK-related processes during proliferative arrest could occur not only through the FUL-AP2 module[9,15], but also through the direct control by FUL.

Discussion

Our study provides an unprecedented detailed characterization of the sequence of molecular and cellular events linked to hormonal regulation, stem cell proliferation and meristem activity that leads to proliferative arrest. In particular, our results show that the onset and progression of this process entails a coordinated temporal repression of CK signaling and CK-dependent processes such as WUS-mediated SAM maintenance, CYCB1;2-promoted cell division, and cell and SAM growth. The early repression of these CK-related processes (3 wab) together with the potential major role of FUL at the time of inflorescence arrest (visible cluster of arrested buds; 4-5 wab) lead us to propose the differentiation of two phases at the end of the flowering period leading to proliferative arrest: a first gradual loss of meristem proliferative capacity and a second short phase that entails complete meristem activity blocking (Figure 7). Importantly, this study will help us to accurately define the framework in future approaches aimed at understanding the molecular basis of this process since, up to now, previous studies at the molecular level[9,14,15] have been exclusively focused on comparisons of high proliferative apices and completely arrested apices, probably missing key information in between both stages. In addition, the parallel characterization performed in *ful* mutant plants suggests that FUL may promote meristem arrest via repression of CK-related pathways. Interestingly, FUL may have two different modes of action in the control of proliferative arrest that correlate with the proposed phases: it would act as a gradual repressor of SAM activity at early stages (mild repressor during the decline) and as a switch that completely inactivates SAM function at later stages (robust repressor during the shutdown) (Figure 7). Our data can be integrated in the model of the temporal regulation of SAM maintenance[9], which proposed that WUS levels in the SAM decreased with age by the action of FUL. FUL promotes proliferative arrest by directly repressing *AP2-like* genes, which maintain SAM activity by promoting *WUS* expression[9]. On the other hand, the reported AP2 regulation of CK response via KMD proteins[15] suggests that AP2 may regulate WUS through this pathway. Thus, our results strengthen previous works and lead to hypothesize, additionally, about alternative pathways downstream of FUL activity regulating CK response and, therefore, SAM activity during the end of flowering (Figure 7). An important goal for future investigation will be to determine the precise molecular mechanisms underlying such differential regulation, whether the decline of CK-related pathways that precedes proliferative arrest could be linked to the concept of arrest-competence proposed by Ware and collaborators[16] and the precise role of FUL in establishing this competence in response to seed-derived or age-related signals[9,16]. Altogether, such approaches will provide a more complete picture of how different factors such as other hormones, environmental signals or age-dependent components proposed in previous

studies[9,14–16] are integrated in this temporal window and control proliferative arrest. For instance, it will be very challenging to study how other hormones previously proposed as proliferative arrest regulators, such as auxins and abscisic acid[14–16], or involved in other developmental stages, such as gibberellins in floral transition[8], are distributed in the SAM during proliferative arrest or whether these hormones interact with CK-related pathways or among them. Finally, since proliferative arrest is common to a wide range of species, the processes described in *Arabidopsis thaliana* might be relevant for further biotechnological approaches aimed at improving yield in crops by optimizing the length of the flowering period. Particularly, because CK treatments prevent meristem arrest and hence extend the fruit production period, CK-related pathways would constitute promising candidate breeding targets.

Acknowledgements

We thank Bruno Müller and Venugopala Reddy for kindly providing the *TCSn:GFP-ER* and *WUS_{pro}:eGFP-WUS* lines, respectively, as well as Vicente Balanzà, Neha Bhatia, Antonio Serrano-Mislata, Concha Gómez-Mena and Francisco Madueño for helpful feedback on the manuscript. Paz Merelo acknowledges Fundación General CSIC (ComFuturo program) for current funding. The laboratory of Cristina Ferrándiz is supported by grants from Ministerio de Ciencia e Innovación (RTI2018-099239-B-I00) and Generalitat Valenciana (PROMETEU/2019/004).

Author contributions

P.M. and C.F. designed the experiments and supervised the project. P.M. and I.G-C. performed the experiments. P.M. analyzed the data and prepared the figures. P.M. and C.F. contributed reagents, materials and analytic tools. P.M. and C.F. wrote the paper.

Declaration of interests

The authors declare no competing interests.

Figure legends

Figure 1. Changes in flower and fruit production, cell size, cell number and meristem size during the flowering period and proliferative arrest. (A) Number of stage 12-15 flowers (asterisks in B) (upper) and total number of mature fruits (lower) produced by the primary SAM along the flowering period and till the proliferative arrest (PA). Data are represented as mean ± SD of 10 biological replicates. Asterisks, $P < 0.0005$, two-tailed Student's *t* test comparing each time point to the previous one. (B) Images of active (2-3 weeks after bolting, wab), arrested (PA normally happens

between 4 and 5 wab) and reactivated apices (1 week after pruning, wap). Asterisks mark the developmental stages of flowers counted in A and black arrowheads point to arrested and dead buds. (C) Heat-map quantification of cell area in the meristem region of active (2-4 wab), arrested (5 wab) and reactivated inflorescence shoot apices (1 wap or 6 wab, 2 wap or 7 wab). Arrested plants were pruned when the PA was observed (5 wab). (D-F) Quantification of cell area (D), cell number (E), and total area (F) of active, arrested and reactivated shoot apical meristems. Data are represented as mean ± SD of 5-8 apices. Letters in D-F represent $P < 0.05$; a, two-tailed Student's *t* test versus the previous time point; b, two-tailed Student's *t* test comparing reactivation (1 wap or 6 wab, 2 wap or 7 wab) to the PA time point (5 wab); c, two-tailed Student's *t* test comparing reactivation (1 wap or 6 wab, 2 wap or 7 wab) to the initial time point (2 wab). Scale bars represent 1 mm (B) and 20 μm (C). See also Figure S1.

Figure 2. CYCB1;2 and CK signaling are repressed during proliferative arrest. (A-J) Expression of *CYCB1;2$_{pro}$:Dbox-GFP* (yellow) in active (A, B, F, G; 2 and 3 wab), arrested (C, H; 4 wab) and reactivated apices (D, I, 1 day after pruning (dap); E, J, 1 wap). Arrested plants were pruned when the PA was observed (4 wab). Cell membranes were highlighted using FM4-64 staining (gray). Confocal projections of the shoot apices combining both CYCB1;2-GFP and FM4-64 channels are shown in A-E. Corresponding projections with the single CYCB1;2-GFP channel are shown in F-J to visualize dividing cells in deeper cell layers. The yellow dashed line outlines primordia and meristems. Pn, flower primordia that have grown out from the meristem; In, incipient primordia. The positions of incipient primordia (In) were predicted from those of existing primordia (Pn). Both primordia and incipient primordia are numbered in order of appearance, starting youngest (P1 or I2) to oldest (P5 or I1). White arrowheads point to less frequent divisions 3 wab (G). Red arrowheads mark dividing cells in the boundaries of active and reactivated apices (F, I). (K) Number of cells expressing CYCB1;2-GFP in the meristem region of active, arrested and reactivated shoot apices. Data are represented as mean ± SD of 5 SAMs. Letters represent $P < 0.005$; a, two-tailed Student's *t* test versus the previous time point; b, two-tailed Student's *t* test comparing reactivation (1 dap, 1 wap or 5 wab) to the PA time point (4 wab); c, two-tailed Student's *t* test comparing reactivation (1 dap, 1 wap or 5 wab) to the initial time point (2 wab). (L) Box plots representing the mean cell area of non-CYCB1;2-GFP expressing cells (CYC-, gray) and CYCB1;2-GFP expressing cells (CYC+, yellow) in the meristem region of five active (2 wab) and reactivated (1 wap or 5 wab) apices. Asterisks indicate a significant difference ($P < 0.05$) from the corresponding CYC- cells according to two-tailed Student's *t* test. (M-Q) Confocal projections of inflorescence shoot apices showing TCSn intensity distribution (magenta; signal intensity calibration bar) 2 (M), 3 (N) and 4 wab (O), and 1 day after pruning (dap) (P) and 1 wap (or 5 wab) (Q). (R-V) Corresponding longitudinal sections of the shoot apices along the dashed lines in M-Q. Cell membranes were highlighted using FM4-64 staining (gray). Green arrowheads point to TCSn signal in the organizing center of the meristem or primordia. White arrowheads mark TCSn expression in the meristem-primordia boundaries. Brightness was

adjusted to the same extent to properly visualize TCSn signal in S, T and U. Scale bars represent 20 μm. See also Figures S2 and S3.

Figure 3. Cytokinins are necessary to prevent and revert proliferative arrest. (A) Quantification of fruits produced by shoot apices of N6-benzylaminopurine (BAP, 100 μM) and mock-treated plants 2 and 5 weeks after the initial treatment (wat) (or 4 and 7 wab, respectively). Inflorescences were treated every 3 days from 2 wab. BAP treatment was stopped 5 wat. Data are shown as mean ± SD of 21 biological replicates treated with BAP or mock. Asterisks indicate a significant difference ($P < 0.001$) from the corresponding mock plants according to two-tailed Student's *t* test. (B-D) Shoot apices 2 weeks after mock (B) and BAP treatment (C), and 5 weeks after BAP treatment (D). (E-G) *TCSn:GFP-ER* expression (magenta) in the shoot apex of mock-treated plants 2 wat (E) and BAP-treated plants 2 and 5 wat (F and G, respectively). (H-J) Corresponding longitudinal sections of the shoot apices along the dashed lines in E-G. (K-N, P-S) TCSn intensity distribution (magenta) 1 day and 1 week after mock (K-N) and 100 μM BAP treatment (P-S) of arrested inflorescences (4 wab, PA). Confocal projections of the shoot apices are shown in K, M, P and R, and the corresponding longitudinal sections marked by the dashed lines are shown in L, N, Q and S. (O, T) Shoot apex of plants that were in PA 1 week after treatment with mock (O) and BAP (T). Cell membranes were highlighted using FM4-64 staining (gray). Weak TCSn signal in control apices (K, L) can be occasionally observed because plant handling during treatments can cause silique and seed dehiscence at late stages and, thus, meristem reactivation. Scale bars represent 1 mm (B-D), 2 mm (O, T) and 20 μm (E-J, K-N, P-S). See also Figure S3.

Figure 4. WUS repression correlates with proliferative arrest. (A-C, F-H) Expression of WUS_{pro}*:eGFP-WUS* (magenta; signal intensity calibration bar) in active (A, B, F, G; 2 and 3 wab) and arrested apices (C, H; 4 wab). Arrested plants were pruned when the PA was observed (4 wab). (D, E, I, J) GFP-WUS expression in apices reactivated by pruning 1 dap (D, I) and 1 wap (E, J). Confocal projections of the shoot apices are shown in A-E, and the corresponding longitudinal sections marked by the dashed lines are shown in F-J. Cell membranes were highlighted using FM4-64 staining (gray). Green arrowheads point to low GFP-WUS signal in the organizing center of the meristem. Scale bars represent 20 μm. See additional time points (days before PA) in Figure S4.

Figure 5. Changes in fruit and flower production, cell area, cell number and meristem area in *ful* shoot apices. (A) Number of flowers at stages 12-15 (asterisks in B) (upper) and total number of mature fruits (lower) produced by the primary SAM in *ful* mutant plants from 2 to 7 wab. Data are represented as mean ± SD of 10 biological replicates. Asterisks, $P < 0.005$, two-tailed Student's *t* test comparing each time point to the previous one. The three distinct phases (high proliferation, transition and low proliferation phase) are indicated. Wild-type data are also shown (dashed line). Significance of wild-type data is represented in Figure 1A. (B) Images of high proliferative apices (1-3 wab), apices at transition (4 and 5 wab) and low proliferative apices (6-7 wab). Asterisks mark the

developmental stages of flowers counted in A. (C) Heat-map quantification of cell area in the meristem region of *ful* shoot apices 2-7 wab. (D–F) Quantification of cell area (D), cell number (E) and meristem area (F) in *ful* meristems 2-7 wab. Data of 4-9 apices are represented. Letters in D-F represent $P < 0.05$; a, two-tailed Student's *t* test versus the previous time point; b, two-tailed Student's *t* test comparing genotypes. Wild-type data from Figures 1D-1F are also shown (light color points). Significance of wild-type data is represented in Figure 1D-F. Phases in C-F are established based on flower and fruit production. Arrested wild-type plants were pruned when the PA was observed (5 wab) and reactivated wild-type SAMs were segmented 1 and 2 wap (that is, 6 and 7 wab). Scale bars represent 1mm (B) and 20 μm (C). See also Figure S5.

Figure 6. Fluctuations in cell divisions, CK signaling and WUS expression correlate with meristem activity changes in *ful* apices. (A-H) Expression of *CYCB1;2$_{pro}$:Dbox-GFP* (yellow) in *ful* apices 2 (A), 3 (B), 4 (C, E), 5 (D, F), 6 (G) and 7 wab (H). Cell membranes were highlighted using FM4-64 staining (gray). Confocal projections of the shoot apices combining both CYCB1;2-GFP and FM4-64 channels are shown in A-H. Corresponding projections with the single CYCB1;2-GFP channel (right panels) are shown to visualize cells in division in deeper cell layers. The yellow dashed line labels primordia and meristems. Pn, flower primordia that have grown out from the meristem; In, incipient primordia (assigned by position). White arrowheads point to less frequent divisions during the transition phase. Red arrowheads mark dividing cells in the boundaries of low proliferative apices. Two degrees of reduction in division were observed in SAMs 4 (C, E) and 5 wab (D, F). (I) Number of cells expressing CYCB1;2-GFP in the meristem region of shoot apices 2 to 7 wab. Data are represented as mean ± SD of 5 SAMs. Letter a indicates a significant difference ($P < 0.005$) from the previous time point according to two-tailed Student's *t* test. (J-O) *TCSn:GFP-ER* expression (magenta) in *ful* apices 2 (J), 3, (K), 4 (L), 5 (M), 6 (N) and 7 wab (O). Confocal projections of the shoot apices are shown in J-O, and the corresponding longitudinal sections marked by the dashed lines are shown in the lower panels. (P-U) Expression of *WUS$_{pro}$:eGFP-WUS* (magenta) in *ful* apices 2 (P), 3 (Q), 4 (R), 5 (S), 6 (T) and 7 wab (U). Confocal projections of the shoot apices are shown in P-U, and the corresponding longitudinal sections marked by the dashed lines are shown in the lower panels. Cell membranes were highlighted using FM4-64 staining (gray). Green arrowheads point to TCSn or GFP-WUS signal in the organizing center. White arrowheads point to TCSn signal in the boundaries. Scale bars represent 20 μm.

Figure 7. Temporal framework of cytokinin-dependent molecular changes that trigger proliferative arrest at the end of the flowering period. Cytokinin regulates SAM size and activity by promoting cell division and WUS expression[38–43,49]. Based on our results, we propose a model in which CK signaling and likely CK levels decrease gradually in the SAM along advanced stages of the reproductive phase. Hence, mitotic divisions decrease in parallel, as shown by the reduction in expression of the G2/M transition marker (CYCB1;2), and also WUS protein levels. Subsequently,

this leads to a reduction in stem cell size and number and, thus, in SAM size[18–20,27,57], as shown by the 2.5D segmentation assay. Repression of these CK-regulated processes causes a gradual decline in SAM activity and flower production and, finally, PA. FUL would promote PA via repression of these CK-dependent pathways. This could be mediated through the AP2-like pathway previously described[9,15]. At early stages (around one week before PA), FUL would contribute, probably together with other factors (X) and seed signals, to reduce the expression domain and levels of CK response factors, CYCB1;2 and WUS (decline). At this point, no new primordia would be generated and the last flowers and fruits would finish to develop. Lastly, FUL would completely block these CK-related pathways and SAM activity (shutdown), as shown by the absence of expression of the fluorescent markers in wild-type SAMs and the recovery in *ful* SAMs. During the shutdown, the inflorescence only contains arrested buds (PA).

STAR Methods

Resource availability

Lead contact

Further information and requests for resources and reagents should be directed to and will be fulfilled by the Lead Contact, Cristina Ferrándiz (cferrandiz@ibmcp.upv.es).

Materials availability

Plasmids and plant materials generated in this study are all available from the Lead Contact upon request. Please note that the distribution of transgenic lines will be governed by material transfer agreements (MTAs) and will be dependent on appropriate import permits acquired by the receiver.

Data and Code Availability

All data reported in this paper will be shared by the lead contact upon request. This paper does not report original code. Any additional information required to reanalyze the data reported in this paper is available from the lead contact upon request.

Experimental model and subject details

Plant material and growth conditions

All plants used in this study were *Arabidopsis thaliana* ecotype Landsberg *erecta* (L*er*). Mutant alleles and transgenic lines have been previously described: *ful-1*[61], *TCSn:GFP-ER*[45] and *WUS*$_{pro}$*:eGFP-WUS*[56]. *TCSn:GFP-ER* and *WUS*$_{pro}$*:eGFP-WUS* lines were crossed to *ful-1* and the experiments were performed with F3 homozygous plants.

Arabidopsis plants were grown in the greenhouse at 21 °C under LD conditions (16 h light), illuminated by cool-white fluorescent lamps (150 µE m^{-2} s^{-1}) and in a 2:1:1 by volume mixture of sphagnum:perlite:vermiculite. To promote germination, seeds were stratified on soil at 4 °C for 3 days in the dark. Plants were watered with a dilution of the Hoagland's nutrient solution 1.

Method details

Plasmid construction and plant transformation

The *CYCB1;2$_{pro}$:Dbox-GFP* transgene was generated based on the previously reported transgene *CYCB1;2$_{pro}$:Dbox-GUS*[28]. A genomic region containing 1147 bp upstream of the *CYCB1;2* transcription start site and 874 bp downstream of the start site, which include the destruction box (Dbox; N-terminal motif that acts as a target for degradation after mitosis), was amplified and cloned into the pCR8 vector using the pCR8/GW/TOPO TA Cloning Kit (Invitrogen). The primers used for amplification were: 5′-GGAGGCCAGAACTTGAAGAAGA-3′ (CYCB1;2_f; forward) and 5′-tAGCACTAAGTACAGACGAGTACGTC-3′ (CYCB1;2_r; reverse). Then, the *CYCB1;2$_{pro}$:Dbox* fragment was cloned into the destination vector pMDC110[62], which contains GFP, by LR recombination (Invitrogen). *Agrobacterium tumefaciens* strain C58 was used to transform *Arabidopsis* wild-type and *ful-1* plants by the floral dip method[63]. The subsequent assays were performed using homozygous transgenic lines carrying a single transgene insertion. We selected T2 lines with an appropriate ratio of segregation on Murashige and Skoog (MS) (Duchefa-Biochemie) plates containing 20 µg/µL hygromycin B (Hyg; Roche). Then, homozygous T3 lines were selected on MS-Hyg plates and imaged under the confocal to identify the brightest lines with the proper cellular expression pattern of *CYCB1;2*[28].

Flower and fruit number quantification

Wild-type and *ful-1* plants grew as described above. Total number of fully elongated fruits produced by the main inflorescence and flowers in stages 12-15 simultaneously present at each time point were quantified for at least ten plants of each genotype. Plants showing health problems or delayed growth were discarded. Quantification was carried out every week from 2 to 7 wab for both genotypes.

Reactivation and hormonal treatments

For reactivation of arrested shoot apices, the rosette-leaf and cauline-leaf branches were cut and all the fruits in the main stem were removed. The lines used for these treatments (wild-type*, TCSn:GFP-ER*, *WUS$_{pro}$:eGFP-WUS* and *CYCB1;2$_{pro}$:Dbox-GFP*) grew at the conditions mentioned above. For each reactivation assay, 10-15 plants of each genotype were used.

After optimization of CK treatments (N6-benzylaminopurine, BAP; Duchefa-Biochemie) (Figure S3), a concentration of 100 μM was used. The BAP stock was prepared in 50 mM NaOH with a final concentration of 50 mM. BAP solution (100 μM BAP, 100 μM NaOH, 0.05% Tween-20) was applied directly to the shoot apices by spraying. Mock solution (100 μM NaOH, 0.05% Tween-20) was used to spray control shoot apices. For continuous BAP treatment (assay of proliferative arrest delay), active apices of 21 *TCSn:GFP-ER* plants were sprayed from 2 wab and every 3 days with BAP or mock solution. For the BAP-mediated reactivation assay, arrested apices (4 wab) of 21 plants *TCSn:GFP-ER* plants were treated with BAP or mock. Quantification of the number of fruits produced by the main stem of BAP and mock-treated plants was carried out as described above.

Confocal microscopy and image analysis

Live imaging analyses were performed on a Zeiss LSM780 confocal microscope (Zeiss, Germany) using a water-dipping 40X objective. Reproductive shoot apices were imaged under water on MS medium plates, and with the stem (length ~4 mm) embedded in the MS medium. To allow a proper exposition of the shoot apex during live imaging, all flower buds were carefully removed with clean tweezers and a fine needle. After dissection, the cell membrane was stained by incubating the dissected apices in FM4-64 (30 μg/mL; Invitrogen) for 15 minutes prior to image. GFP was imaged using an argon laser emitting at the wavelength of 488 nm together with a 499-527 nm collection. To image FM4-64 a DPSS 561-10 laser emitting at 561 nm was used together with a 666-759 nm collection. GFP/FM4-64 combination was imaged using the conditions mentioned for each channel and sequential scanning in line-scan mode with a MBS 488/561 filter. Z-stacks were acquired with a resolution of 8 or 12-bit depth, section spacing of 0.5-0.8 mm and line averaging of 2. At least two experiments were conducted by transgenic line (*TCSn:GFP-ER*, *WUS_{pro}:eGFP-WUS*, *$CYCB1;2_{pro}$:Dbox-GFP, TCSn:GFP-ER_ful-1*, *WUS_{pro}:eGFP-WUS_ful-1* and *$CYCB1;2_{pro}$:Dbox-GFP_ful-1)* where more than five shoot apical meristems were observed. GFP gain was set up equally for all the samples analyzed for each time course. Finally, the acquired z-stacks from the confocal microscope were analyzed using Fiji Image J[64] (https://fiji.sc/) to obtain maximum intensity projections images and optical sections. Brightness was only modified for the proper visualization of *$CYCB1;2_{pro}$:Dbox-GFP*-expressing cells. GFP fluorescence intensity (signal heat-map) was also measured in Fiji.

2.5D segmentation analysis

Cell area, cell number and SAM area of wild-type (2-5 wab, and 1 and 2 wap) and *ful-1* (2-7 wab) shoot meristems were quantified using the MorphoGraphX (MGX) software[26] (https://morphographx.org/). SAM z-stacks were acquired with a z-step of 0.5 mm and converted to TIF files with Fiji. The surface of the SAM was extracted and subdivided, and the FM4-64 signal of

the cell membrane from the L1 cells was projected onto the mesh created. The 2D curved image generated was segmented into cells using automatic seeding and watershed segmentation (radius of 2 μm). Then, cells were manually corrected. To detect the boundaries between the meristem and the developing primordia, the geometry of the surface layer was shown as Gaussian curvatures (neighboring radius of 10 μm). Primordia delimited by cells with negative Gaussian curvature values were manually removed, as well as cells at the boundaries (see Figure S1). Finally, the area heat-maps of the segmented meristem regions were generated.

Quantification and statistical analysis

All statistical analyses were performed using Microsoft Excel software. Significance of data represented in Figures 1-3, 5, 6 and S3 was determined by two-tailed Student's *t* test.

References

1. Hensel, L.L., Nelson, M.A., Richmond, T.A., and Bleecker, A.B. (1994). The fate of inflorescence meristems is controlled by developing fruits in Arabidopsis. Plant Physiol. *106*, 863–876.
2. Lockhart, J.A., and Gottschall, V. (1961). Fruit-induced & apical senescence in Pisum sativum L. Plant Physiol. *36*, 389–398.
3. Murneek, A.E. (1926). Effects of correlation between vegetative and reproductive functions in the tomato (Lycopersicon esculentum Mill.). Plant physiol. *1*, 3-56.7.
4. Kinoshita, A., and Richter, R. (2020). Genetic and molecular basis of floral induction in Arabidopsis thaliana. J. Exp. Bot. *71*, 2490–2504.
5. Huijser, P., and Schmid, M. (2011). The control of developmental phase transitions in plants. Development *138*, 4117–4129.
6. Andrés, F., and Coupland, G. (2012). The genetic basis of flowering responses to seasonal cues. Nat. Rev. Genet. *13*, 627–639.
7. Hyun, Y., Richter, R., and Coupland, G. (2017). Competence to flower: Age-controlled sensitivity to environmental cues. Plant Physiol. *173*, 36–46.
8. Kinoshita, A., Vayssières, A., Richter, R., Sang, Q., Roggen, A., Van Driel, A.D., Smith, R.S., and Coupland, G. (2020). Regulation of shoot meristem shape by photoperiodic signaling and phytohormones during floral induction of Arabidopsis. eLife *9*, 1–29.
9. Balanzà, V., Martínez-Fernández, I., Sato, S., Yanofsky, M.F., Kaufmann, K., Angenent, G.C., Bemer, M., and Ferrándiz, C. (2018). Genetic control of meristem arrest and life span in Arabidopsis by a FRUITFULL-APETALA2 pathway. Nat. Commun. *9*, 565.
10. Balanzà, V., Martínez-Fernández, I., Sato, S., Yanofsky, M.F., and Ferrándiz, C. (2019). Inflorescence meristem fate is dependent on seed development and FRUITFULL in Arabidopsis thaliana. Front. Plant Sci. *10*, 1622–1622.

11. Brand, U., Fletcher, J.C., Hobe, M., Meyerowitz, E.M., and Simon, R. (2000). Dependence of stem cell fate in Arabidopsis on a feedback loop regulated by CLV3 activity. Science *289*, 617 LP – 619.
12. Laux, T., Mayer, K.F., Berger, J., and Jurgens, G. (1996). The WUSCHEL gene is required for shoot and floral meristem integrity in Arabidopsis. Development *122*, 87–96.
13. Mayer, K.F.X., Schoof, H., Haecker, A., Lenhard, M., Jürgens, G., and Laux, T. (1998). Role of WUSCHEL in regulating stem cell fate in the Arabidopsis shoot meristem. Cell *95*, 805–815.
14. Wuest, S.E., Philipp, M.A., Guthörl, D., Schmid, B., and Grossniklaus, U. (2016). Seed production affects maternal growth and senescence in Arabidopsis. Plant Physiol. *171*, 392–404.
15. Martínez-Fernández, I., de Moura, S.M., Alves-Ferreira, M., Ferrándiz, C., and Balanzà, V. (2020). Identification of players controlling meristem arrest downstream of the FRUITFULL-APETALA2 pathway. Plant Physiol. *184*, 945–959.
16. Ware, A., Walker, C.H., Šimura, J., González-Suárez, P., Ljung, K., Bishopp, A., Wilson, Z.A., and Bennett, T. (2020). Auxin export from proximal fruits drives arrest in temporally competent inflorescences. Nat. Plants *6*, 699–707.
17. Goetz, M., Rabinovich, M., and Smith, H.M. (2021). The role of auxin and sugar signaling in dominance inhibition of inflorescence growth by fruit load. Plant Physiol. *187*, 1189–1201.
18. Gaillochet, C., Stiehl, T., Wenzl, C., Ripoll, J.J., Bailey-Steinitz, L.J., Li, L., Pfeiffer, A., Miotk, A., Hakenjos, J.P., Forner, J., et al. (2017). Control of plant cell fate transitions by transcriptional and hormonal signals. eLife *6*, 1–30.
19. Jones, A.R., Forero-Vargas, M., Withers, S.P., Smith, R.S., Traas, J., Dewitte, W., and Murray, J.A.H. (2017). Cell-size dependent progression of the cell cycle creates homeostasis and flexibility of plant cell size. Nat. Commun. *8*, 1–13.
20. Laufs, P., Grandjean, O., Jonak, C., Kiêu, K., and Traas, J. (1998). Cellular parameters of the shoot apical meristem in Arabidopsis. Plant Cell *10*, 1375–1389.
21. Serrano-Mislata, A., Schiessl, K., and Sablowski, R. (2015). Active control of cell size generates spatial detail during plant organogenesis. Curr. Biol. *25*, 2991–2996.
22. Bodson, M. (1975). Variation in the rate of cell division in the apical meristem of Sinapis alba during transition to flowering. Ann. Bot. *39*, 547–554.
23. Jacqmard, A., Gadisseur, I., and Bernier, G. (2003). Cell division and morphological changes in the shoot apex of Arabidopsis thaliana during floral transition. Ann. Bot. *91*, 571–576.
24. Kwiatkowska, D. (2008). Flowering and apical meristem growth dynamics. J. Exp. Bot. *59*, 187–201.
25. Marc, J., and Palmer, J.H. (1982). changes in mitotic activity and cell size in the apical meristem of Helianthus annuus L. during the transition to flowering. Am. J. Bot. *69*, 768–775.
26. Barbier de Reuille, P., Routier-Kierzkowska, A.-L., Kierzkowski, D., Bassel, G.W., Schüpbach, T., Tauriello, G., Bajpai, N., Strauss, S., Weber, A., Kiss, A., et al. (2015). MorphoGraphX: A platform for quantifying morphogenesis in 4D. eLife *4*, 5864–5864.

27. Kondorosi, E., Roudier, F., and Gendreau, E. (2000). Plant cell-size control: Growing by ploidy? Curr. Opin. Plant Biol. *3*, 488–492.
28. Donnelly, P.M., Bonetta, D., Tsukaya, H., Dengler, R.E., and Dengler, N.G. (1999). Cell cycling and cell enlargement in developing leaves of Arabidopsis. Dev. Biol. *215*, 407–419.
29. Gutierrez, C. (2009). The Arabidopsis cell division cycle. TAB *7*, e0120–e0120.
30. Louveaux, M., Julien, J.-D., Mirabet, V., Boudaoud, A., and Hamant, O. (2016). Cell division plane orientation based on tensile stress in Arabidopsis thaliana. Proc. Natl. Acad. Sci. USA *113*, E4294–E4303.
31. Reddy, G.V., Heisler, M.G., Ehrhardt, D.W., and Meyerowitz, E.M. (2004). Real-time lineage analysis reveals oriented cell divisions associated with morphogenesis at the shoot apex of Arabidopsis thaliana. Development *131*, 4225–4237.
32. Shapiro, B.E., Tobin, C., Mjolsness, E., and Meyerowitz, E.M. (2015). Analysis of cell division patterns in the *Arabidopsis* shoot apical meristem. Proc. Natl. Acad. Sci. USA *112*, 4815–4820.
33. Gan, S. (2003). Mitotic and postmitotic senescence in plants. Sci. Aging Knowledge Environ. *2003*, RE7.
34. Noodén, L.D., Guiamét, J.J., and John, I. (2004). 15 - Whole plant senescence. In, L. D. B. T.-P. C. D. P. Noodén, ed. (Academic Press), pp. 227–244.
35. Ha, C.M., Jun, J.H., and Fletcher, J.C. (2010). Chapter Four - Shoot apical meristem form and function. In Plant Development, M. C. P. B. T.-C. T. in D. B. Timmermans, ed. (Academic Press), pp. 103–140.
36. Murray, J.A.H., Jones, A., Godin, C., and Traas, J. (2012). Systems analysis of shoot apical meristem growth and development: Integrating hormonal and mechanical signaling. Plant Cell *24*, 3907–3919.
37. Soyars, C.L., James, S.R., and Nimchuk, Z.L. (2016). Ready, aim, shoot: stem cell regulation of the shoot apical meristem. Curr. Opin. Plant Biol. *29*, 163–168.
38. Schaller, G.E., Street, I.H., and Kieber, J.J. (2014). Cytokinin and the cell cycle. Curr. Opin. Plant Biol. *21*, 7–15.
39. Bartrina, I., Otto, E., Strnad, M., Werner, T., and Schmülling, T. (2011). Cytokinin regulates the activity of reproductive meristems, flower organ size, ovule formation, and thus seed yield in Arabidopsis thaliana. Plant Cell *23*, 69–80.
40. Li, X.G., Su, Y.H., Zhao, X.Y., Li, W., Gao, X.Q., and Zhang, X.S. (2010). Cytokinin overproduction-caused alteration of flower development is partially mediated by CUC2 and CUC3 in Arabidopsis. Gene *450*, 109–120.
41. Del Pozo, J.C., Lopez-Matas, M.A., Ramirez-Parra, E., and Gutierrez, C. (2005). Hormonal control of the plant cell cycle. Physiol. Plant. *123*, 173–183.
42. Jelenska, J., Deckert, J., Kondorosi, E., and Legocki, A. (2000). Mitotic B-type cyclins are differentially regulated by phytohormones and during yellow lupine nodule development. Plant Sci. *150*, 29–39.

733 43. Yang, W., Cortijo, S., Korsbo, N., Roszak, P., Schiessl, K., Gurzadyan, A., Wightman, R.,
734 Jönsson, H., and Meyerowitz, E. (2021). Molecular mechanism of cytokinin-activated cell division in
735 Arabidopsis. Science *371*, 1350–1355.
736 44. Liu, J., and Müller, B. (2017). Imaging TCSn::GFP, a synthetic cytokinin reporter, in Arabidopsis
737 thaliana BT - Plant Hormones: Methods and Protocols. In, J. Kleine-Vehn and M. Sauer, eds.
738 (Springer New York), pp. 81–90.
739 45. Zürcher, E., Tavor-Deslex, D., Lituiev, D., Enkerli, K., Tarr, P.T., and Müller, B. (2013). A robust
740 and sensitive synthetic sensor to monitor the transcriptional output of the cytokinin signaling network
741 in planta. Plant Physiol. *161*, 1066–1075.
742 46. Higuchi, M., Pischke, M.S., Mähönen, A.P., Miyawaki, K., Hashimoto, Y., Seki, M., Kobayashi,
743 M., Shinozaki, K., Kato, T., Tabata, S., et al. (2004). In planta functions of the Arabidopsis cytokinin
744 receptor family. Proc. Natl. Acad. Sci. USA *101*, 8821–8826.
745 47. Miyawaki, K., Tarkowski, P., Matsumoto-Kitano, M., Kato, T., Sato, S., Tarkowska, D., Tabata, S.,
746 Sandberg, G., and Kakimoto, T. (2006). Roles of Arabidopsis ATP/ADP isopentenyltransferases and
747 tRNA isopentenyltransferases in cytokinin biosynthesis. Proc. Natl. Acad. Sci. USA *103*, 16598–
748 16603.
749 48. Werner, T., Motyka, V., Laucou, V., Smets, R., Van Onckelen, H., and Schmülling, T. (2003).
750 Cytokinin-deficient transgenic Arabidopsis plants show multiple developmental alterations indicating
751 opposite functions of cytokinins in the regulation of shoot and root meristem activity. Plant Cell *15*,
752 2532–2550.
753 49. Gordon, S.P., Chickarmane, V.S., Ohno, C., and Meyerowitz, E.M. (2009). Multiple feedback
754 loops through cytokinin signaling control stem cell number within the Arabidopsis shoot meristem.
755 Proc. Natl. Acad. Sci. USA *106*, 16529–16534.
756 50. Kim, H.J., Chiang, Y.-H., Kieber, J.J., and Schaller, G.E. (2013). SCF(KMD) controls cytokinin
757 signaling by regulating the degradation of type-B response regulators. Proc. Natl. Acad. Sci. USA
758 *110*, 10028–10033.
759 51. Ferreira, F.J., and Kieber, J.J. (2005). Cytokinin signaling. Curr. Opin. Plant Biol. *8*, 518–525.
760 52. Haberer, G., and Kieber, J.J. (2002). Cytokinins. New insights into a classic phytohormone. Plant
761 Physiol. *128*, 354–362.
762 53. Kieber, J.J., and Schaller, G.E. (2018). Cytokinin signaling in plant development. Development
763 *145*, dev149344.
764 54. Meng, W.J., Cheng, Z.J., Sang, Y.L., Zhang, M.M., Rong, X.F., Wang, Z.W., Tang, Y.Y., and
765 Zhang, X.S. (2017). Type-B ARABIDOPSIS RESPONSE REGULATORs specify the shoot stem cell
766 niche by dual regulation of WUSCHEL. Plant Cell *29*, 1357–1372.
767 55. Leibfried, A., To, J.P.C., Busch, W., Stehling, S., Kehle, A., Demar, M., Kieber, J.J., and Lohmann,
768 J.U. (2005). WUSCHEL controls meristem function by direct regulation of cytokinin-inducible
769 response regulators. Nature *438*, 1172–1175.
770 56. Yadav, R.K., Perales, M., Gruel, J., Girke, T., Jönsson, H., and Venugopala Reddy, G. (2011).

WUSCHEL protein movement mediates stem cell homeostasis in the Arabidopsis shoot apex. Genes Dev. *25*, 2025–2030.

57. Yadav, R.K., Tavakkoli, M., and Reddy, G.V. (2010). WUSCHEL mediates stem cell homeostasis by regulating stem cell number and patterns of cell division and differentiation of stem cell progenitors. Development *137*, 3581–3589.

58. Bemer, M., Van Mourik, H., Muiño, J.M., Ferrándiz, C., Kaufmann, K., and Angenent, G.C. (2017). FRUITFULL controls SAUR10 expression and regulates Arabidopsis growth and architecture. J. Exp. Bot. *68*, 3391–3403.

59. Werner, T., Motyka, V., Strnad, M., and Schmülling, T. (2001). Regulation of plant growth by cytokinin. Proc. Natl. Acad. Sci. USA *98*, 10487–10492.

60. Werner, T., and Schmülling, T. (2009). Cytokinin action in plant development. Curr. Opin. Plant Biol. *12*, 527–538.

61. Gu, Q., Ferrandiz, C., Yanofsky, M.F., and Martienssen, R. (1998). The FRUITFULL MADS-box gene mediates cell differentiation during Arabidopsis fruit development. Development *125*, 1509–1517.

62. Curtis, M.D., and Grossniklaus, U. (2003). A gateway cloning vector set for high-throughput functional analysis of genes in planta. Plant Physiol. *133*, 462–469.

63. Clough, S.J., and Bent, A.F. (1998). Floral dip: a simplified method for Agrobacterium-mediated transformation of Arabidopsis thaliana. Plant J. *16*, 735–743.

64. Schneider, C., Rasband, W. and Eliceiri, K. (2012). NIH Image to ImageJ: 25 years of image analysis. Nat. Methods *9*, 671–675.

Figure 1

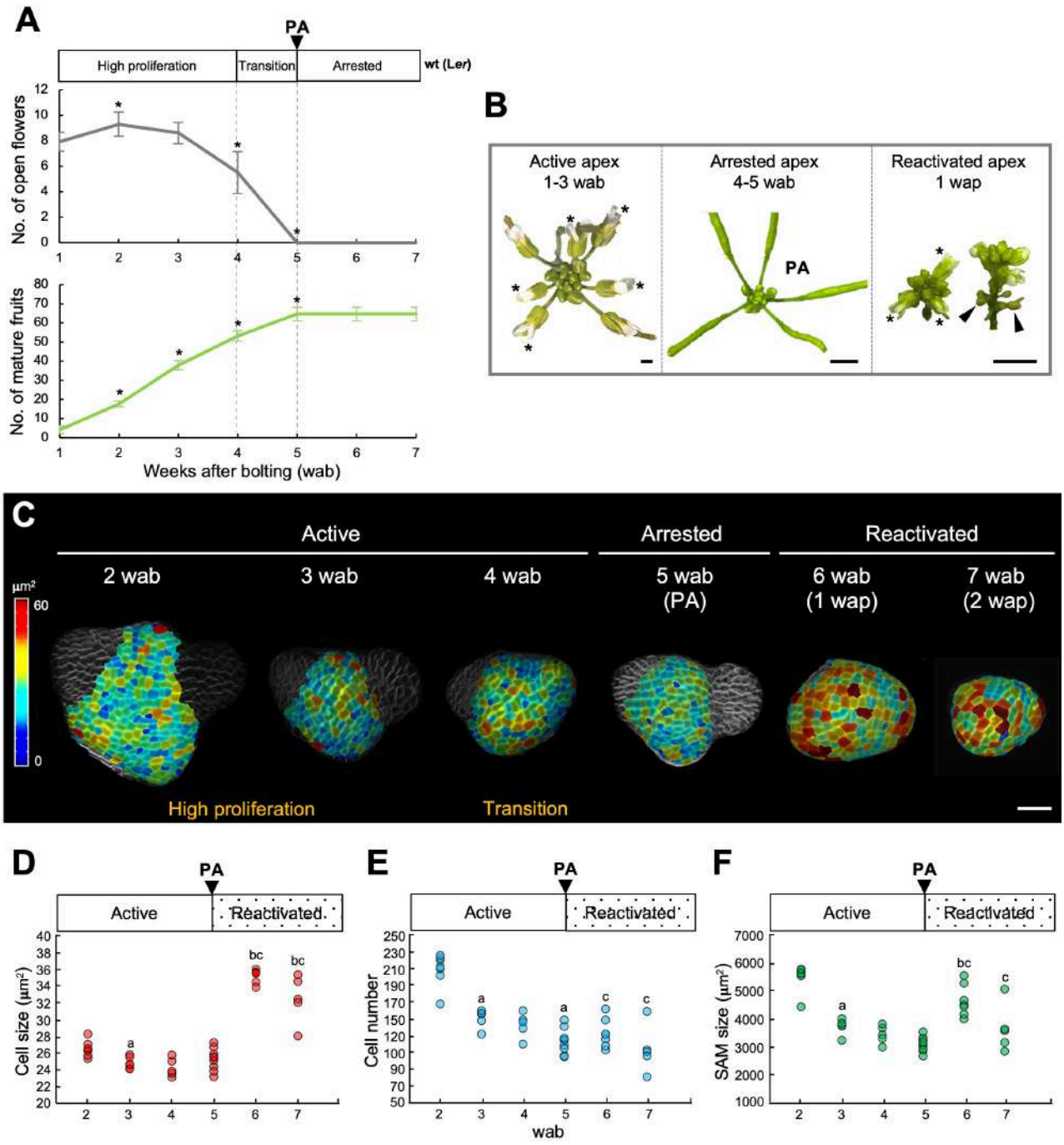
A
PA
High proliferation
Transition
Arrested
wt (Ler)
No. of open flowers
No. of mature fruits
Weeks after bolting (wab)
B
Active apex
1-3 wab
Arrested apex
4-5 wab
Reactivated apex
1 wap
PA
C
Active
Arrested
Reactivated
2 wab
3 wab
4 wab
5 wab
(PA)
6 wab
(1 wap)
7 wab
(2 wap)
µm²
60
0
High proliferation
Transition
D
PA
Active
Reactivated
Cell size (µm²)
E
PA
Active
Reactivated
Cell number
wab
F
PA
Active
Reactivated
SAM size (µm²)

Figure 2

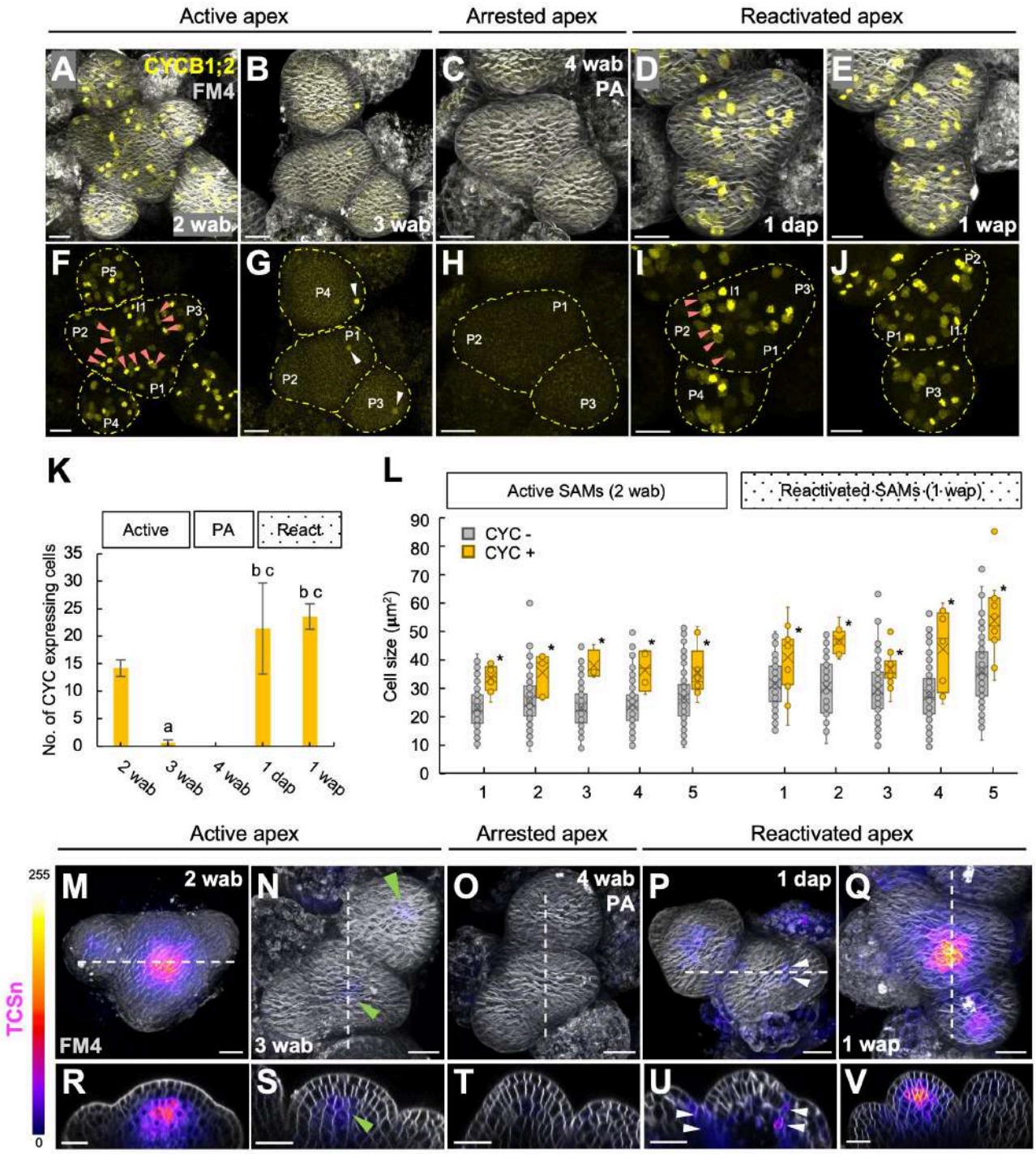
Active apex
Arrested apex
Reactivated apex
A
CYCB1;2
FM4
2 wab
B
3 wab
C
4 wab
PA
D
1 dap
E
1 wap
F
P5
I1
P3
P2
P1
P4
G
P4
P1
P2
P3
H
P1
P2
P3
I
I1
P3
P2
P1
P4
J
P2
P1
I1
P3
K
Active
PA
React
No. of CYC expressing cells
35
30
25
20
15
10
5
0
a
b c
b c
2 wab
3 wab
4 wab
1 dap
1 wap
L
Active SAMs (2 wab)
Reactivated SAMs (1 wap)
CYC -
CYC +
Cell size (µm²)
90
80
70
60
50
40
30
20
10
0
1
2
3
4
5
1
2
3
4
5
Active apex
Arrested apex
Reactivated apex
255
TCSn
0
M
2 wab
FM4
N
3 wab
O
4 wab
PA
P
1 dap
Q
1 wap
R
S
T
U
V

Figure 3

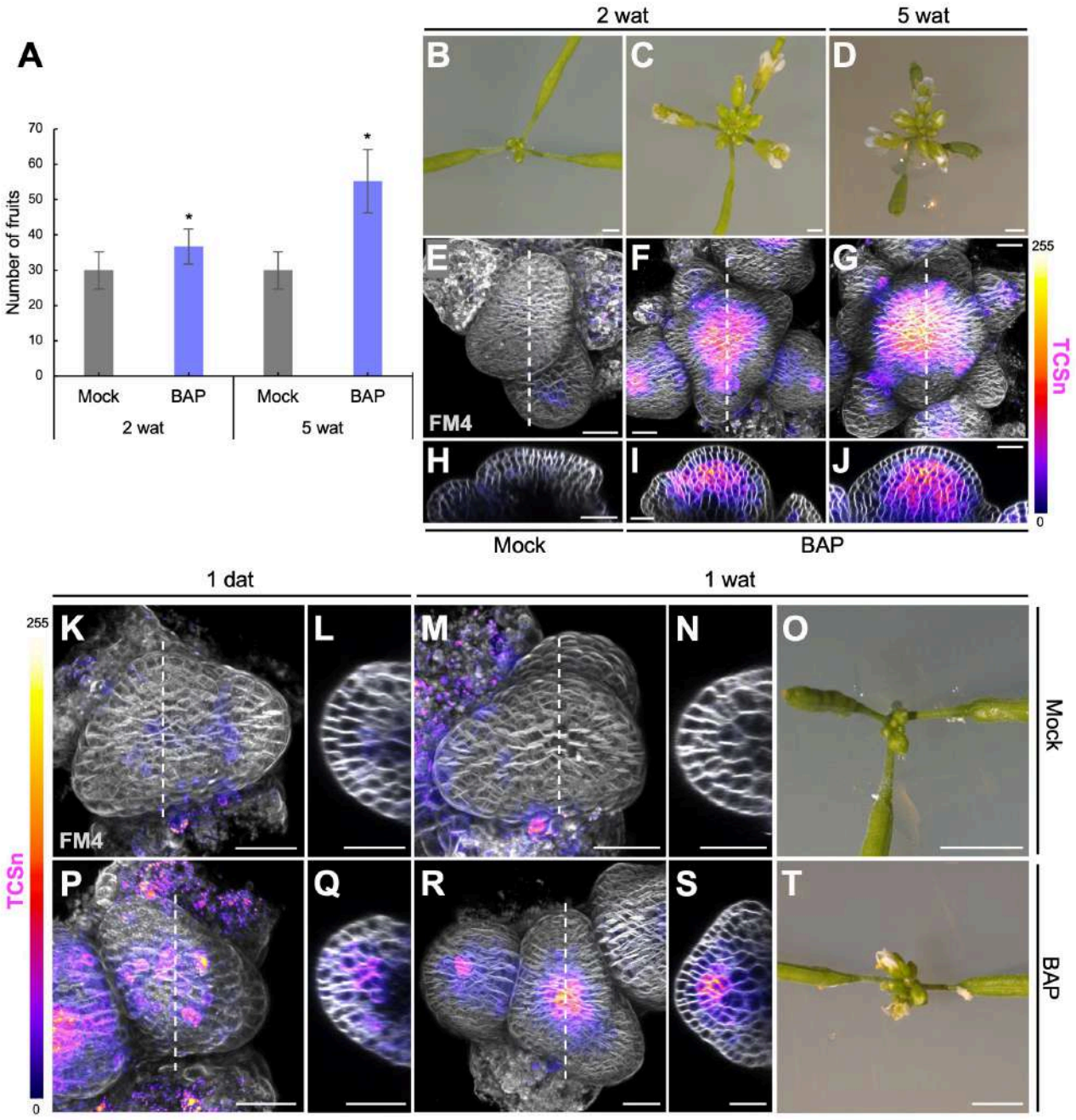
A
Number of fruits
70
60
50
40
30
20
10
0
Mock
BAP
Mock
BAP
2 wat
5 wat
2 wat
5 wat
B
C
D
E
F
G
H
I
J
FM4
255
TCSn
0
Mock
BAP
1 dat
1 wat
K
L
M
N
O
P
Q
R
S
T
FM4
255
TCSn
0
Mock
BAP

Figure 4

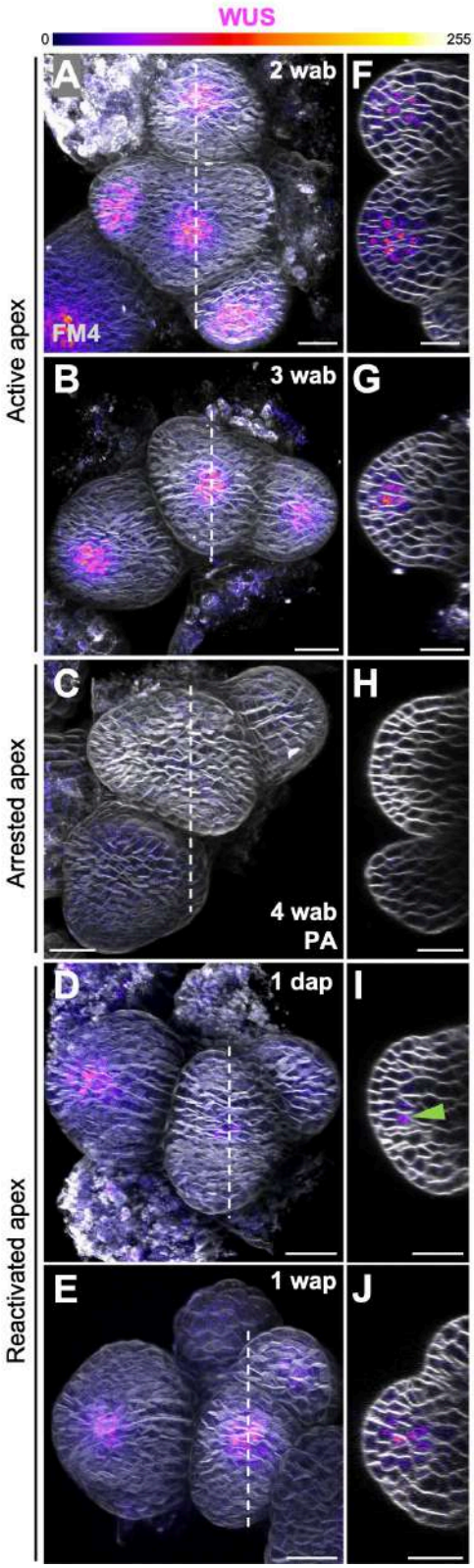
WUS
0
255
A
2 wab
F
FM4
B
3 wab
G
C
H
4 wab
PA
D
1 dap
I
E
1 wap
J
Active apex
Arrested apex
Reactivated apex

Figure 5

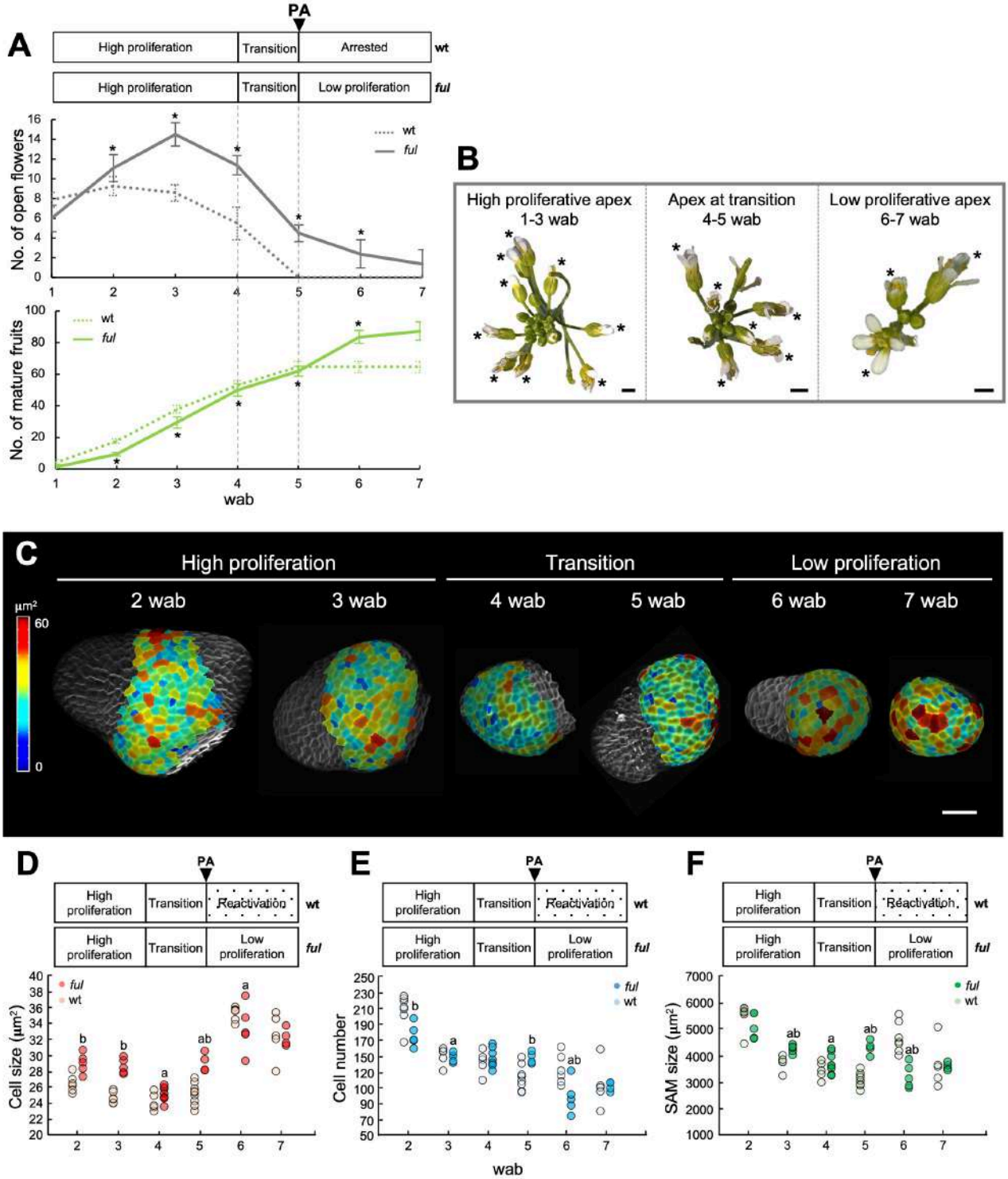
A
PA
High proliferation
Transition
Arrested
wt
High proliferation
Transition
Low proliferation
ful
No. of open flowers
No. of mature fruits
wab
B
High proliferative apex
1-3 wab
Apex at transition
4-5 wab
Low proliferative apex
6-7 wab
C
High proliferation
Transition
Low proliferation
2 wab
3 wab
4 wab
5 wab
6 wab
7 wab
µm²
60
0
D
E
F
Reactivation
Cell size (µm²)
Cell number
SAM size (µm²)
ful
wt
wab

Figure 6

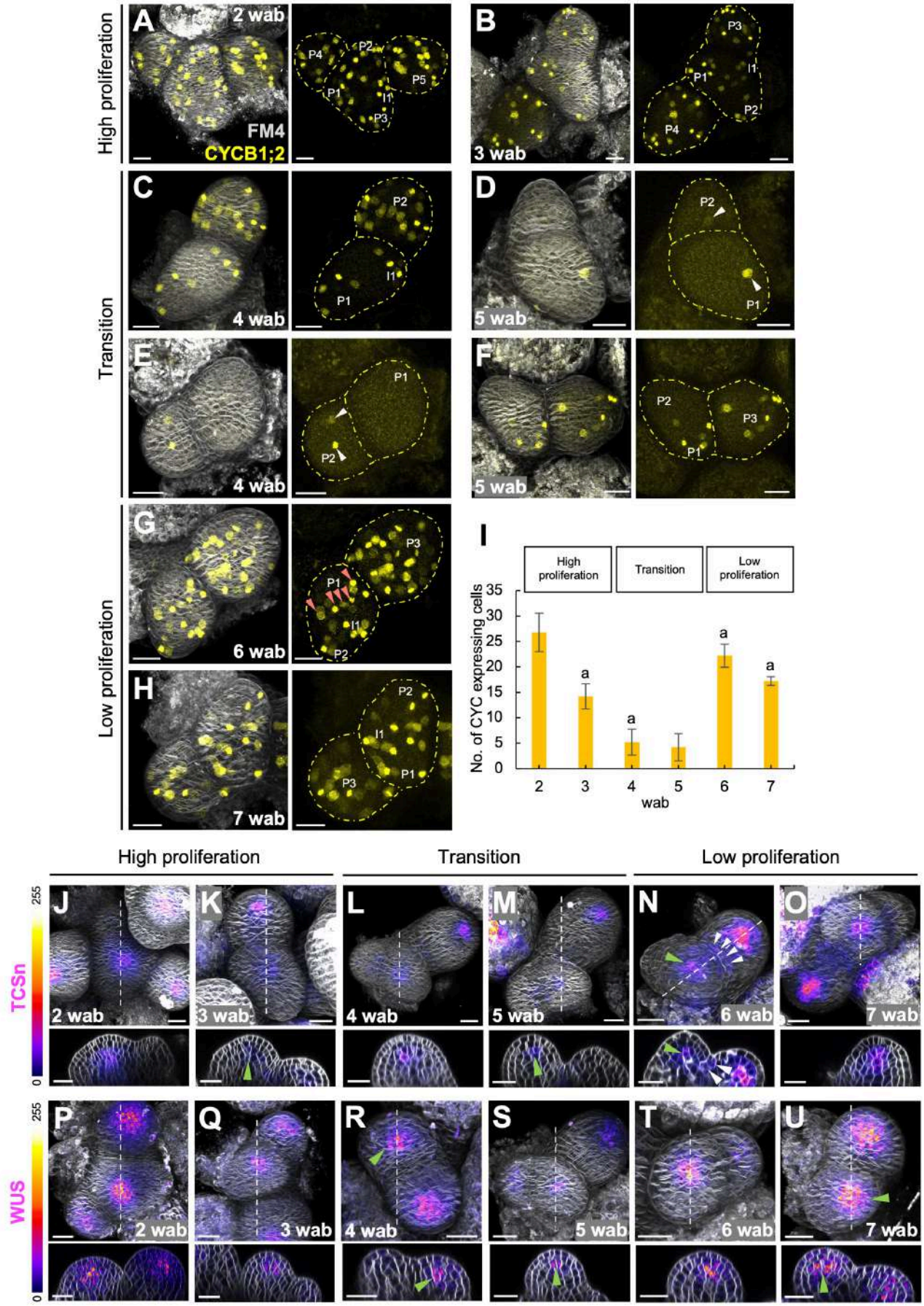
High proliferation
Transition
Low proliferation
A
2 wab
FM4
CYCB1;2
B
3 wab
C
4 wab
D
5 wab
E
4 wab
F
5 wab
G
6 wab
H
7 wab
I
No. of CYC expressing cells
wab
J
K
L
M
N
O
TCSn
P
Q
R
S
T
U
WUS

Figure 7

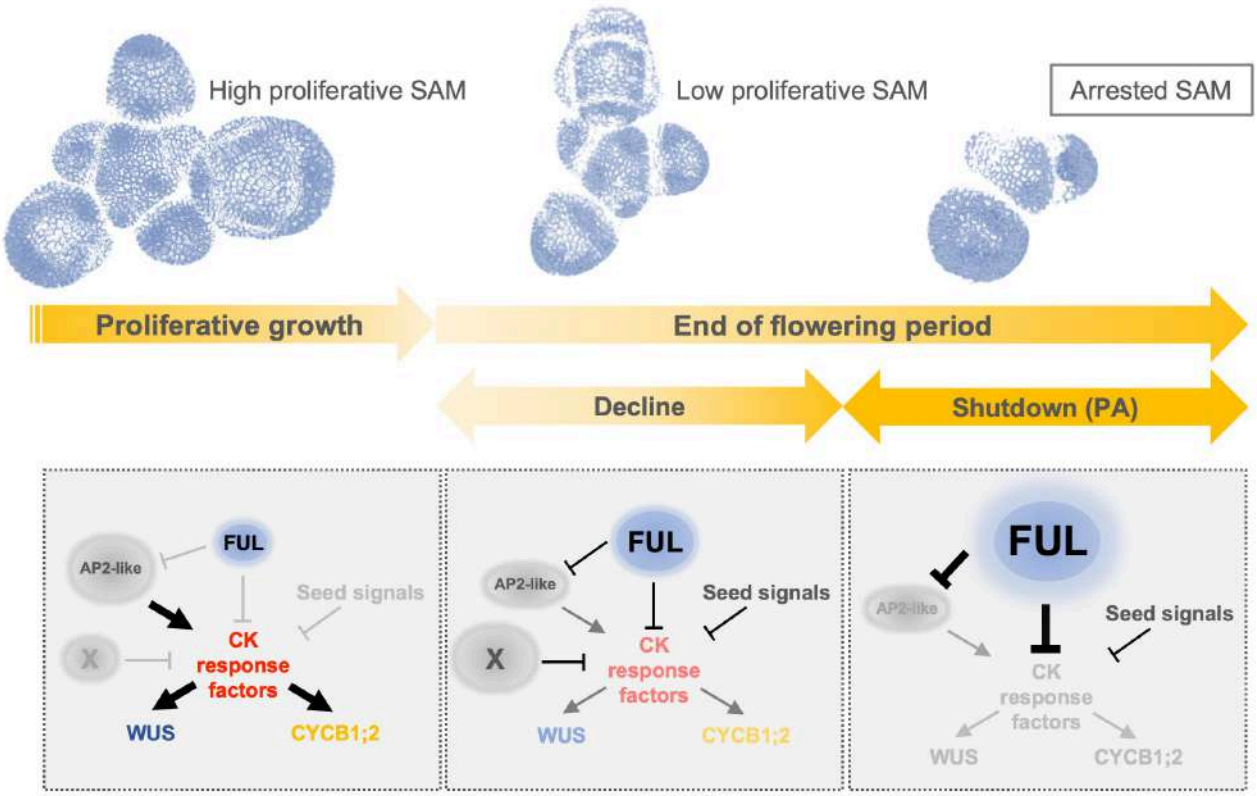
High proliferative SAM
Low proliferative SAM
Arrested SAM
Proliferative growth
End of flowering period
Decline
Shutdown (PA)
AP2-like
FUL
Seed signals
X
CK
response
factors
WUS
CYCB1;2

Supplemental information

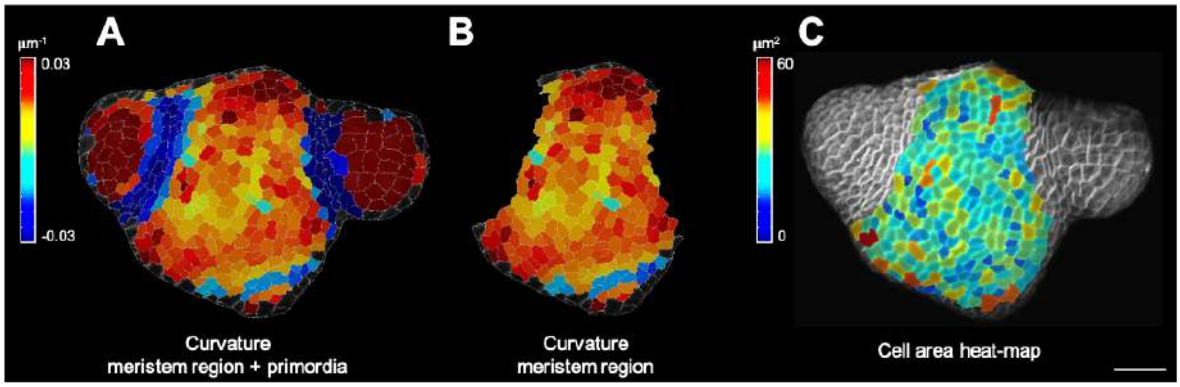

Figure S1. 2.5D Segmented surface projection of a shoot apex. Related to Figure 1. (A) Gaussian curvature allows to delimit the primordia that have grown out from the meristem region (cells with negative values mark the meristem-primordia boundaries). (B) Meristem region isolation after discarding the primordia. For convenience, we considered that a primordium has grown out from the meristem when the boundary is completely filled by blue cells. (C) Cell area heat-map extracted after segmentation. Cell membranes were stained with FM4-64 (gray) to allow segmentation. Scale bar represents 20 μm.

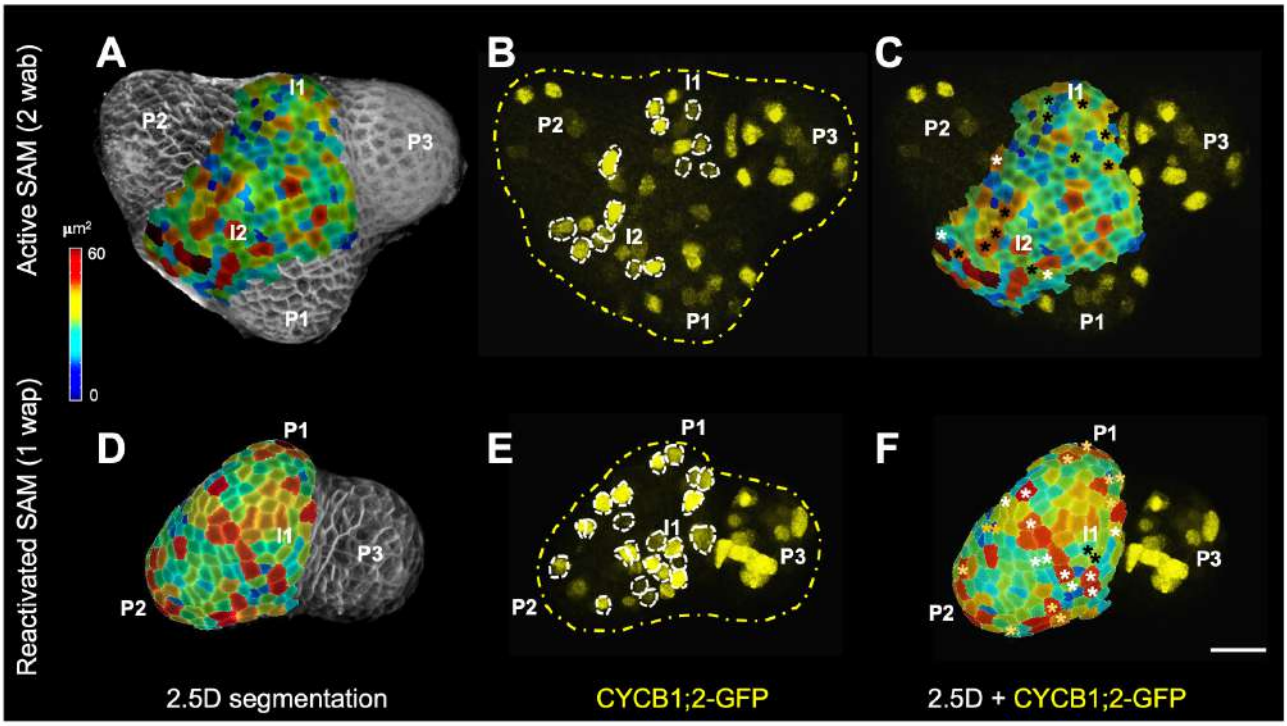

G

Active SAMs (2 wab)	Cell area CYC - (μm^2)	Cell area CYC + (μm^2)	p-value
1	23.1	33.8	6.8E-06
2	25.5	35.5	1.7E-02
3	23.3	38.1	8.4E-03
4	24.2	36.4	4.5E-02
5	26.4	35.6	1.6E-02
Reactivated SAMs (1 wap)			
1	31.5	40.9	6.2E-03
2	30.4	46.7	1.9E-06
3	29.5	36.7	9.2E-05
4	27.6	43.9	1.3E-02
5	35.9	53.8	1.8E-03

Figure S2. Correlation between cell divisions and cell area. Related to Figure 2. (A, D) Cell area heat-map of an active (A; 2 wab) and a reactivated SAM (D; 1 wap) of *CYCB1;2$_{pro}$:Dbox-GFP* expressing plants. Cell membrane staining with FM4-64 (gray) allowed segmentation. (B, E) Expression of *CYCB1;2$_{pro}$:Dbox-GFP* (yellow) in the same SAMs shown in A and D. (C, F) Combination of the cell area heat-map and the CYCB1;2-GFP channel (yellow) to identify the epidermal dividing cells along the heat-map mesh. The yellow dashed line outlines primordia and meristem. The white dashed line marks epidermal dividing cells. White asterisks mark dividing cells in the boundaries, yellow asterisks represent dividing cells in primordia and black asterisks point to dividing cells in incipient primordia. Pn, flower primordia that have grown out from the meristem; In,

961 incipient primordia (assigned by position). Scale bar represents 20 μm. (G) Data plotted in Figure
962 2L.
963
964
965
966
967
968
969
970
971
972
973
974
975
976
977
978
979
980
981
982
983
984
985
986
987
988
989
990
991
992
993
994
995

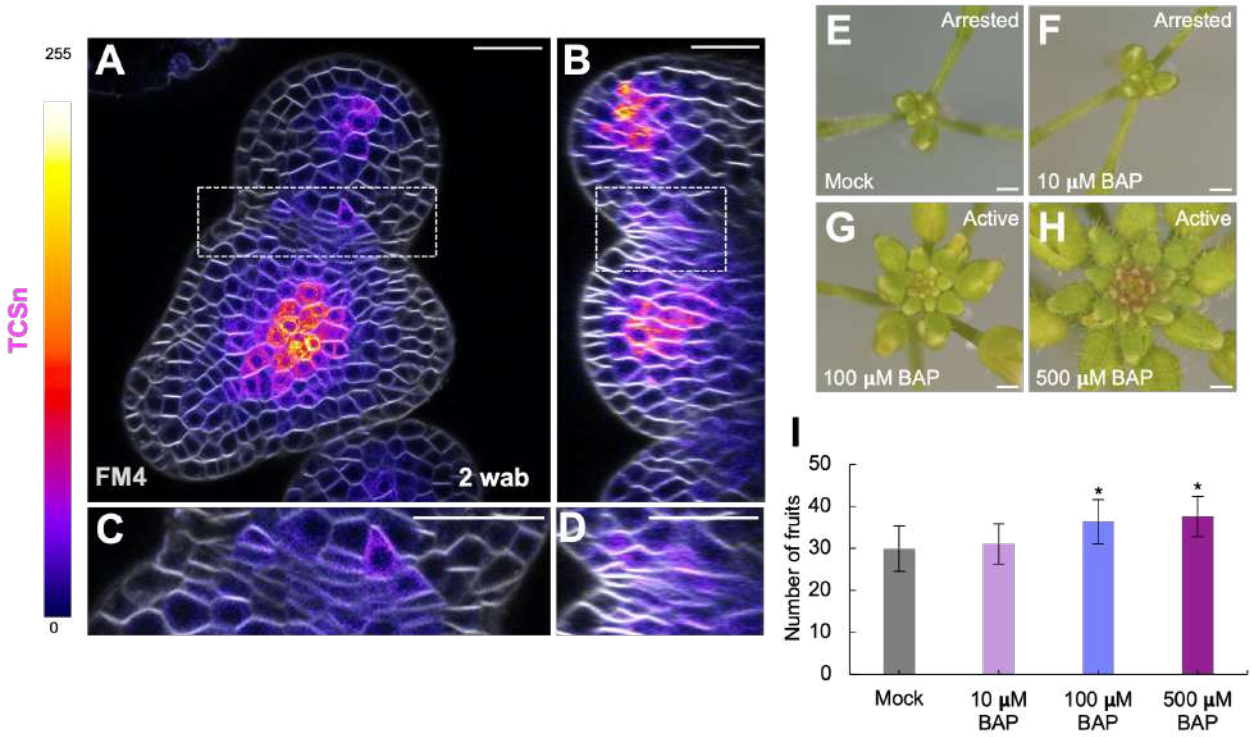

Figure S3. TCSn expression at the meristem-primordia boundaries. Related to Figures 2 and 3, and STAR Methods. (A, B) Cross (A) and longitudinal sections (B) of a shoot apex showing TCSn:GFP-ER intensity distribution (magenta) 2 wab. (C, D) Corresponding magnified images of the boundaries marked by the dashed squares in A and B. Cell membranes were highlighted using FM4-64 staining (gray). Brightness was slightly increased in the GFP channel by Fiji to visualize TCSn expression at the boundaries. (E-I) Optimization of CK treatment**.** Shoot apices 2 weeks after mock treatment (E; arrested) or treatment with 10 (F; arrested), 100 (G; active) or 500 μM (H; active) N6-benzylaminopurine (BAP). Inflorescences were treated every 3 days from 2 wab. (I) Quantification of fruits produced by shoot apices of BAP (10, 100 or 500 μM) and mock-treated plants 2 weeks after treatment (or 4 wab). Data are shown as mean ± SD of 20 biological replicates treated with BAP or mock. Asterisks indicate a significant difference ($P < 0.001$) from the corresponding mock plants according to two-tailed Student's *t* test. Scale bars represent 20 μm (A-D) and 0.5 mm (E-H).

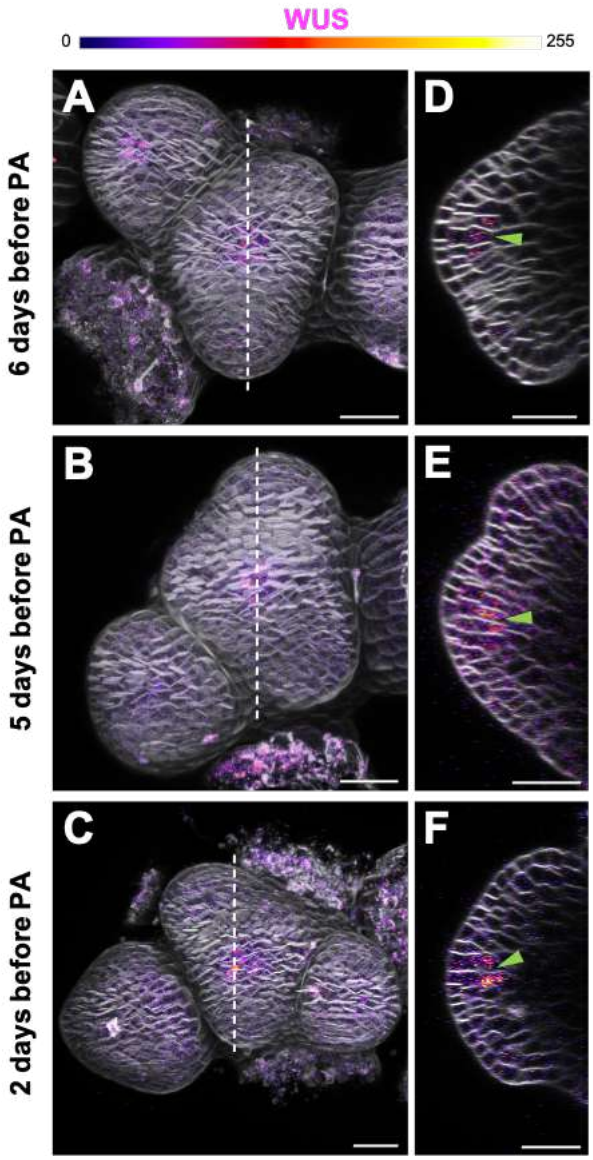

Figure S4. WUS expression is repressed a few days before proliferative arrest. Related to Figure 4. (A, C) Confocal projections of the shoot apices showing *WUS*$_{pro}$*:eGFP-WUS* expression (magenta; signal intensity calibration bar) 6 (A), 5 (B) and 2 days before PA (C). (D, E, F) Corresponding longitudinal sections marked by the dashed lines in A, B and C. Cell membranes were highlighted using FM4-64 staining (gray). Green arrowheads point to low GFP-WUS signal in the organizing center of the meristem. Images were acquired using a laser gain higher than the gain used for the images shown in Figures 4 and 6 (1065-1080 instead of 950) to detect the very low levels of GFP-WUS signal at these time points. Scale bars represent 20 μm.

Figure S5. *ful* mutant plant at an advanced stage of the flowering period. Related to Figure 5.

The upper part of the main stem of *ful* plants 11 wab is shown. The shoot apex is shown in the magnified image. Scale bar represents 1 mm.